Keynote Topic

This article is part of the **Materials Informatics** keynote topic compilation.

Symmetry-Based Computational Tools for Magnetic Crystallography

J.M. Perez-Mato,[1] S.V. Gallego,[1] E.S. Tasci,[2] L. Elcoro,[1] G. de la Flor,[1] and M.I. Aroyo[1]

[1]Departamento de Física de la Materia Condensada, Facultad de Ciencia y Tecnología, Universidad del País Vasco, UPV/EHU, 48080 Bilbao, Spain; email: jm.perez-mato@ehu.es

[2]Department of Physics Engineering, Hacettepe University, 06800 Ankara, Turkey

Annu. Rev. Mater. Res. 2015. 45:217–48

First published online as a Review in Advance on March 30, 2015

The *Annual Review of Materials Research* is online at matsci.annualreviews.org

This article's doi: 10.1146/annurev-matsci-070214-021008

Keywords

magnetic crystallography, Bilbao Crystallographic Server, magnetic structure determination, magnetic space groups, magnetic symmetry software, magnetic superspace symmetry

Abstract

In recent years, two important advances have opened new doors for the characterization and determination of magnetic structures. Firstly, researchers have produced computer-readable listings of the magnetic or Shubnikov space groups. Secondly, they have extended and applied the superspace formalism, which is presently the standard approach for the description of nonmagnetic incommensurate structures and their symmetry, to magnetic structures. These breakthroughs have been the basis for the subsequent development of a series of computer tools that allow a more efficient and comprehensive application of magnetic symmetry, both commensurate and incommensurate. Here we briefly review the capabilities of these computation instruments and present the fundamental concepts on which they are based, providing various examples. We show how these tools facilitate the use of symmetry arguments expressed as either a magnetic space group or a magnetic superspace group and allow the exploration of the possible magnetic orderings associated with one or more propagation vectors in a form that complements and goes beyond the traditional representation method. Special focus is placed on the programs available online at the Bilbao Crystallographic Server (**http://www.cryst.ehu.es**).

1. INTRODUCTION

MSG: magnetic space group, also called Shubnikov group

MSSG: magnetic superspace group

Representation method: method to parameterize and determine magnetic structures using basis functions adapted to the *irreps* of the space group of the paramagnetic phase

***Irrep*:** irreducible representation of a group

Magnetic ordering is a symmetry-breaking process, and, as in other fields of physics, the characterization of the involved symmetry reduction is an essential step for its comprehension. The symmetry of a magnetic phase is given by a magnetic space group (MSG) (also called a Shubnikov group) (1, 2), if commensurate, or by a magnetic superspace group (MSSG) (3–5), in the case of an incommensurate ordering. The symmetry group of a magnetic phase determines all structural and magnetic symmetry constraints that are thermodynamically obliged within its whole stability range. These symmetry-dictated properties can only be broken through an additional phase transition or by applying a symmetry-breaking perturbation. By comparing the symmetry group of a magnetic phase with the symmetry group of the parent paramagnetic phase, one can also determine the set of possible domains and twin-related configurations. The symmetry characterization of magnetic phases, expressed in the form of a symmetry group, is especially important for predicting and understanding their magneto-structural properties. Furthermore, similar to what happens in conventional crystallography, the assignment of some symmetry to a magnetic structure implies very specific constraints on the possible magnetic moments and atomic positions, which can be unambiguously defined and distinguished from other features that are not symmetry protected.

The identification of the relevant magnetic symmetry and its constraints can therefore be considered an essential part of the characterization of a magnetic phase. However, magnetic symmetry considerations have been absent from most studies for decades because of the lack of computer-readable listings of MSGs and computational tools based on magnetic symmetry. In contrast, Bertaut (6, 7), and later Izyumov's group (8–11), developed the so-called representation method, and free efficient software was soon available for its application (12–14). Thus, the representational analysis has become the most popular method for determining and describing magnetic structures. In this method, the possible magnetic orderings are parameterized using spin modes, which transform according to one or more irreducible representations (*irreps*) of the space group of the paramagnetic phase. In the more general case of multidimensional *irreps*, this method neither uses nor controls the magnetic symmetry of the spin configurations. Therefore, magnetic structures are commonly reported without assigning any magnetic symmetry. In the case of incommensurate phases, this situation was inevitable, as ordinary MSGs are not applicable, and the specific use of superspace symmetry and MSSGs for magnetic structures was not considered in detail and translated into appropriate software until recently (4). In these circumstances, despite some early attempts (15), no comprehensive database of magnetic structures exists yet, although hundreds of such structures are reported each year. The development of such a database requires an unambiguous and unified description of magnetic structures and demands a systematic application of magnetic symmetry information. Also, the renewed interest in multiferroics in the past decade (16–19), for which symmetry-governed magneto-structural properties are especially important, has evidenced the need for a more comprehensive use of magnetic symmetry concepts.

In this context, a considerable number of free computational tools for the analysis of magnetic structures based on and/or applying magnetic symmetry have been developed during the past few years. Computer-readable listings of MSG data are now available, whereas refinement programs have been implemented in which models constrained by alternative possible MSGs or MSSGs can be derived and tested. These are complemented by various programs that allow the analysis of possible magnetic orderings for a given parent structure, with full consideration of symmetry properties, consistently including both magnetic symmetry groups and *irreps*. This novel extensive software has opened a new path in which magnetic symmetry is employed as a tool to both enumerate possible alternative magnetic models and store and retrieve, in a robust, unambiguous,

and unified form, any magnetic structure, commensurate or incommensurate. Furthermore, under the auspices of the International Union of Crystallography, the CIF (crystallographic information file) dictionary (20) is being extended to magnetic structures (21). The new symmetry-based computational tools use this so-called magCIF file format (in its preliminary form), which has also been adopted by some visualization programs. These developments have already permitted the creation of an incipient small database of commensurate and incommensurate magnetic structures, in which magnetic symmetry (in the form of an MSG or MSSG) is employed (22).

Here we briefly review these computation instruments, with a short introduction to their theoretical basis and some examples of their applications. We give special attention to the computer tools that have been developed by our group, namely those available at the Bilbao Crystallographic Server (23, 24).

Below, we use the Seitz notation for any symmetry operation as defined in Reference 25 but extended to magnetic groups by including time reversal with the symbol $1'$ and writing any point-group operation $\mathbf{R}$ combined with time reversal as $\mathbf{R}'$. The transformations to different bases or settings are expressed in the shorthand notation used in the *International Tables for Crystallography* (26). Following common practice in the field, the terms magnetic moment and spin are used here indistinctly as synonyms. Full information on the magnetic structures discussed below can be found in MAGNDATA (22), the aforementioned collection of magnetic structures, which is freely available on the Internet. Structure figures have been produced using either VESTA (27) or Jmol (28).

CIF: crystallographic information file; standard text file format for crystallographic data exchange developed and sponsored by the International Union of Crystallography

magCIF: extension of the crystallographic information file format to magnetic structures (under development)

Gray group: MSG of a paramagnetic phase; it includes the time reversal operation with zero translation

2. COMMENSURATE MAGNETIC STRUCTURES

2.1. Magnetic Space Groups (Shubnikov Groups)

In the context of magnetic structures, average atomic magnetic moments can be considered real quantities, and the action of the time reversal operation simply changes the sign of all atomic magnetic moments in the structure while keeping unchanged the nonmagnetic degrees of freedom. By definition, a commensurately ordered magnetic phase breaks the time reversal symmetry operation that is present in the magnetically disordered paramagnetic phase. If G is the space group of the paramagnetic phase, its full symmetry, considering the presence of the disordered atomic spins, is given by the gray magnetic group $G1'$, which can be decomposed in *cosets* as $G1' = G + \{1' \mid 0, 0, 0\}G$. Thus, the full symmetry group of the system includes, in addition to the operations of G, those obtained by multiplying all of them with $\{1' \mid 0, 0, 0\}$ (i.e., the time reversal operation with zero translation). The symmetry of a commensurately magnetically ordered phase is then described by a subgroup of this parent group $G1'$, say Ω, where $\{1' \mid 0, 0, 0\}$ is necessarily absent. This means that the MSG Ω may include nonidentity operations either combined or not combined with time reversal, but not both. Being commensurate, the lattice or a sublattice of the paramagnetic phase will also be maintained, and in general, Ω can be decomposed in *cosets* with respect to a subgroup F of G with the same lattice periodicity as Ω in one of the following three forms: $\Omega = F$, $\Omega = F + \{\mathbf{R_o}' \mid \mathbf{t}\}F$, or $\Omega = F + \{1' \mid \mathbf{L}\}\, F$, where $\{\mathbf{R_o}' \mid \mathbf{t}\}$ and $\{1' \mid \mathbf{L}\}$ are operations of the gray group $G1'$, and $\mathbf{L}$ is a specific lattice translation of the paramagnetic phase. For consistency, $\{\mathbf{R_o} \mid \mathbf{t}\}^2$ and $\{1 \mid 2\mathbf{L}\}$ must belong to F, whereas $\{\mathbf{R_o} \mid \mathbf{t}\}$ and $\{1 \mid \mathbf{L}\}$ belong to G but not to F. These three types of possible magnetic symmetry breakings correspond to the three types of MSGs known as type I, III, and IV, respectively (1, 2) (type II are the gray groups). Notice that all the symmetry operations present in MSGs of type I coincide with those of the ordinary space groups, but as magnetic groups, the existence within the symmetry of the system of the same operations combined with time reversal is explicitly discarded. Thus, for

example, a paramagnetic phase with space group *Pnma* can transform into a magnetic phase with MSG *Pnma* as the result of a symmetry breaking $Pnma1' \rightarrow Pnma$, where all symmetry operations combined with time reversal, which are implicitly present in the paramagnetic phase, disappear.

Effective space group *H*: space group that defines the symmetry constraints on atomic positions of a commensurate magnetic structure; it can be derived from the structure's MSG

OG notation: standard notation for an MSG in which the unit cell used is the one of the effective space group *H*

BNS notation: standard notation of an MSG in which the unit cell used defines the lattice periodicity of the magnetic structure

As stressed in the introduction, the constraints coming from the MSG of a magnetic phase are robust (symmetry-protected) properties within the whole phase. Both atomic magnetic moments and atomic positions are subjected to it. Any operation $\{\mathbf{R}' \mid \mathbf{t}\}$, which includes time reversal, acts on the atomic positions in the same way as the operation $\{\mathbf{R} \mid \mathbf{t}\}$ without time reversal; therefore, the effective symmetry that constrains the atomic positions can be described by an effective space group H, which is either F, $F + \{\mathbf{R_o} \mid \mathbf{t}\}F$, or $F + \{1 \mid \mathbf{L}\}F$, depending on Ω being type I, III, or IV, respectively. In addition, the symmetry relations forced by the magnetic group on the atomic magnetic moments can be reduced to the following rule: If two atoms with nonzero magnetic moments have their atomic positions related by an operation of Ω, then their moments are related by the corresponding point-group operation $\mathbf{R}$ (transforming as axial vectors) with an additional change of sign if time reversal is included in the operation. For magnetic atoms at special positions, i.e., kept invariant by some of the operations of Ω, site-symmetry restrictions on the possible magnetic moments exist, and they are part of the definition of the Wyckoff positions of an MSG.

Litvin (29) recently tabulated the 1,651 mathematically distinct MSGs (1, 2) in a form analogous to that of the ordinary space groups in the *International Tables for Crystallography* (30). These tables of MSGs are freely available electronically and use the so-called Opechowski-Guccione (OG) description (31). This notation employs the space group H, defined above, as the reference to describe the symmetry operations, and therefore, in the case of type IV groups, the employed unit cell does not generate the lattice of the magnetic configuration. This is the essential difference with the alternative Belov-Neronova-Smirnova (BNS) description (32), in which the employed unit cell defines the lattice periodicity of the spin arrangement. Computer-readable tables of MSG data have been produced by Stokes & Campbell (33) in both the BNS and OG notations. Online retrieval tools at the Bilbao Crystallographic Server, based on these tables, allow access to the symmetry operations (MGENPOS) and Wyckoff positions (MWYCKPOS) of any chosen MSG (34). All these listings and tools keep the same conventions, and therefore they can be taken as standard. The MSGs in this review are given in BNS notation.

The MSG Ω defining the symmetry of a commensurate magnetic phase can be introduced without making any reference to the gray space group $G1'$ defining the symmetry of its paramagnetic phase. In fact, the same group Ω, as a mathematical group type, can be relevant for different parent $G1'$ groups. But, as in other ferroics, the domain and switching properties of the system are only defined if the parent group $G1'$ is also known. Therefore, a full description of the symmetry properties of a magnetic phase requires the knowledge of both symmetries: $G1'$ and its subgroup Ω. More concretely, if H is the effective space group of the nonmagnetic degrees of freedom, described above, and s is its index with respect to G (i.e., the factor relating the number of operations in G and H), then $2s$ is the index of Ω with respect to $G1'$, and one can choose s operations $\{g_j\}$ of G (*coset* representatives) not belonging to H, such that $G = H + g_2H + \cdots + g_sH$, and s equivalent, distinct, domain-related structures can be obtained by applying each operation g_j to the magnetic structure. An additional set of s trivially related domains, with reversed moments, corresponds to the application of the symmetry operations g_j'. The magnetic symmetry of a domain-related structure obtained by the action of g_j is given by the subgroup $g_j\Omega g_j^{-1}$ of $G1'$. This subgroup can coincide with Ω or be a distinct subgroup belonging to the same conjugacy class. Conjugate subgroups describe physically equivalent symmetry breakings. Below, if nothing is said to the contrary, an MSG Ω is implicitly taken as a representative of a class of conjugate subgroups with respect to a parent space group $G1'$.

Table 1 Operations that define the MSG of the magnetic structure of $GdMn_2O_5$[a]

N	(x, y, z)[b]	(m_x, m_y, m_z)[c]	Seitz notation
1	$x, y, z, +1$	m_x, m_y, m_z	$\{1 \mid 0, 0, 0\}$
2	$-x + 3/4, y + 1/2, -z, +1$	$-m_x, m_y, -m_z$	$\{2_{010} \mid 3/4, 1/2, 0\}$
3	$-x + 1/4, y + 1/2, z, +1$	$m_x, -m_y, -m_z$	$\{m_{100} \mid 1/4, 1/2, 0\}$
4	$x + 1/2, y, -z, +1$	$-m_x, -m_y, m_z$	$\{m_{001} \mid 1/2, 0, 0\}$
5	$x + 1/2, y, z, -1$	$-m_x, -m_y, -m_z$	$\{1' \mid 1/2, 0, 0\}$
6	$-x + 1/4, y + 1/2, -z, -1$	$m_x, -m_y, m_z$	$\{2'_{010} \mid 1/4, 1/2, 0\}$
7	$-x + 3/4, y + 1/2, z, -1$	$-m_x, m_y, m_z$	$\{m'_{100} \mid 3/4, 1/2, 0\}$
8	$x, y, -z, -1$	$m_x, m_y, -m_z$	$\{m'_{001} \mid 0, 0, 0\}$

Abbreviation: MSG, magnetic space group.

[a]These operations (modulo lattice translations) are a subset of those in *Pbam*1′, expressed in a setting $(2\mathbf{a}_p, \mathbf{b}_p, \mathbf{c}_p; 0, 0, 0)$, where $\{\mathbf{a}_p, \mathbf{b}_p, \mathbf{c}_p\}$ is the parent *Pbam*1′ basis. They define a subgroup of *Pbam*1′, which is the polar MSG P_aca2_1 (#29.104), but in a nonstandard setting (see text).

[b]Operations are expressed in the usual crystallographic notation, but with the addition of the symbol −1/+1 to indicate the combination or not with time reversal.

[c]Transformation of a generic spin (m_x, m_y, m_z) associated with the general position (x, y, z).

2.2. Crystallographic Description of Commensurate Magnetic Structures

Following an approach similar to the one employed for nonmagnetic crystal structures, once the MSG is defined through its set of operations and its unit cell, a magnetic structure is unambiguously described by listing the atomic positions and magnetic moments of a set of symmetry-independent atoms within the unit cell, the so-called asymmetric unit. As an example, **Tables 1** and **2** describe the magnetic structure of $GdMn_2O_5$ (35), also shown in **Figure 1*a***. The directions of the spins (not explicitly given in the original reference) are only approximate. **Tables 1** and **2**, together with the unit cell parameters, are the essential information included in a magCIF file, and they

Table 2 Symmetry-independent atoms of the magnetic structure of $GdMn_2O_5$

Label	Atom type	x^a	y^a	z^a	Symmetry constraints on M	M_x[b]	M_y[b]	M_z[b]	$\lvert M \rvert$
Gd1_1	Gd	0.06975	0.17160	0.00000	$m_x, m_y, 0$	4.87	1.63	0.0	5.14
Gd1_2	Gd	0.93025	0.82840	0.00000	$m_x, m_y, 0$	−4.51	−1.5	0.0	4.75
Mn1	Mn	0.00000	0.50000	0.25510	m_x, m_y, m_z	−2.85	0.95	0.0	3.00
Mn2_1	Mn	0.20590	0.35180	0.50000	$m_x, m_y, 0$	3.8	−1.27	0.0	4.01
Mn2_2	Mn	0.79410	0.64820	0.50000	$m_x, m_y, 0$	3.8	−1.27	0.0	4.01
O1	O	0.00000	0.00000	0.26970					
O2_1	O	0.07630	0.44860	0.00000					
O2_2	O	0.92370	0.55140	0.00000					
O3_1	O	0.07270	0.43560	0.50000					
O3_2	O	0.92730	0.56440	0.50000					
O4_1	O	0.19970	0.20760	0.24500					
O4_2	O	0.80030	0.79240	0.24500					

Abbreviations, ICSD, Inorganic Crystal Structure Database; a blank cell denotes not applicable.

[a]Approximate atomic positions have been taken from entry 97046 of the ICSD (36, 37) and are given in the basis $(2\mathbf{a}_p, \mathbf{b}_p, \mathbf{c}_p; 0, 0, 0)$, with $\mathbf{a}_p, \mathbf{b}_p, \mathbf{c}_p$ being the parent *Pbam* basis.

[b]Approximate magnetic moment components (μB) have been estimated from the model reported in Reference 35.

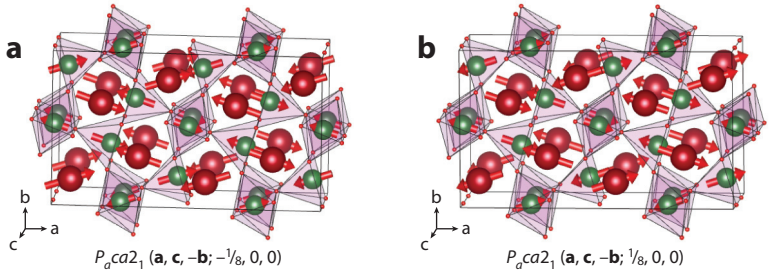

Figure 1

(*a*) Magnetic structure of $GdMn_2O_5$ (35) described in **Tables 1** and **2**. (*b*) Twin structure equivalent to panel *a*. The two configurations must have opposite, magnetically induced polarizations. Their symmetry is given by different but conjugate magnetic space groups indicated below.

are sufficient for the unambiguous definition of the atomic positions and moments of the whole structure. They can be generated from the atomic positions and moments listed in **Table 2** using the symmetry operations of **Table 1**. The MSG in **Table 1** is in a nonstandard setting, using a basis as close as possible to the one of the parent phase. The symmetry operations of all MSGs are freely available in a standard form in the references mentioned above, and therefore, the information in **Table 1** could be substituted with just the label of this MSG: P_aca2_1 (#29.104), together with the transformation from the employed unit cell basis (and origin) to the standard setting of the group. This transformation is indicated in **Figure 1** in a shorthand notation (26). Applying the inverse of this transformation to the operations of the standard MSG available in References 33 or 34, one can directly obtain the operations listed in **Table 1**. Below, we define any relevant magnetic subgroup by this means, i.e., with its standard BNS label plus a transformation to its standard setting.

Table 2 shows that the spin model reported for $GdMn_2O_5$ in Reference 35 has simplifying features that are not symmetry forced: Namely, the Mn1 moment is constrained to lie on the plane *ab*, whereas the spins of the two independent Mn2_1 and Mn2_2 sites are restricted to be exactly equal. Although these restrictions may be reasonable, it is important to have them clearly separated from the fundamental ones that are symmetry protected and are evidenced in **Table 2**. Lacking more precise details, the atomic positions listed in **Table 2** are those of the paramagnetic phase (36, 37) and therefore comply with the parent space group *Pbam* (#55), but the table shows that some atomic sites are split because of the symmetry reduction. Hence, in principle, these split sites could vary their positions independently within the magnetic phase if magneto-structural couplings are sufficiently large. Also, the Mn1 site, which does not split, transforms into a general position, with its three coordinates becoming free. Even if these new structural degrees of freedom triggered by the magnetic ordering remain negligible within experimental resolution, it is convenient to be aware of them. They are fundamental for monitoring any possible structural distortion induced by the magnetic ordering. The effective space group that governs the triggering of new structural degrees of freedom with respect to the paramagnetic phase is given by the operations listed in **Table 1**, disregarding the presence of time reversal in the operation. This is the space group $Pmc2_1$ (#26) in a nonstandard setting and with a centered unit cell doubled along *a*, the transformation to standard setting being (**c**, −**a**/2, −**b**; 3/8, 0, 0) [this can be directly obtained with the IDENTIFY GROUP tool in the Bilbao Crystallographic Server (38)]. This effective space group for the atomic positions is the space group that we have generically called *H* above. The magnetic ordering therefore implies for the atomic positional structure an effective

symmetry breaking: $Pbam \rightarrow Pmc2_1$ ($Pb2_1m$ in the setting used) without change of lattice. This is a transformation from a nonpolar phase to a polar one, with the polar axis along the *b* direction of the parent setting. According to the von Neumann principle, an induced electric polarization P_y should be expected.

Antitranslation: translation combined with time reversal

Thus, without making appeal to any specific mechanism, the symmetry characterization of the magnetic structure allows one to infer that the system will behave as a multiferroic of type II, with a magnetically induced ferroelectricity (16, 18), in agreement with experimental evidence (35). Interestingly, researchers have proposed a similar spin model for $PrMn_2O_5$ (40), but these authors explicitly discard the existence of an electric polarization. The symmetry of the proposed magnetic ordering is, however, coincident with the one above, and some induced ferroelectricity, however small, is to be expected.

The index of the MSG of $GdMn_2O_5$ with respect to the parent symmetry $Pbam1'$ is four. Thus, two distinct twin-related configurations exist, apart from their corresponding trivial twins with all spins reversed. The second nontrivial twin is shown in **Figure 1*b***. This configuration can be obtained by transforming the structure shown in **Figure 1*a*** with any lost operation of the parent space group *Pbam*. This means any operation of the second *coset* in the *coset* decomposition of *Pbam* with respect to its subgroup $Pmc2_1$ ($\mathbf{c}, -\mathbf{a}/2, -\mathbf{b}; 3/8, 0, 0$), such as the inversion operation $\{-1 \mid 0, 0, 0\}$: $Pbam = Pmc2_1 + \{-1 \mid 0, 0, 0\}Pmc2_1$. These operations switch the structural polarity, and therefore the two magnetic domains will have opposite orientations of P_y. Notice that the magnetic symmetry of the second domain-related configuration is given by a different MSG (specified in **Figure 1*b***).

The online editing tools ISOCIF (41) and STRCONVERT (42) are very useful in the field of describing and building up commensurate magnetic structures with full application of magnetic symmetry. They can be used to produce or edit the magCIF file of any real or hypothetical magnetic structure. If the MSG of a given magnetic structure is unknown, a model with all atomic positions and spins in the unit cell can be introduced or edited under the trivial symmetry *P*1. The actual magnetic symmetry of the structure and a description in accordance with it can then be obtained [the program FINDSYM (43) is applied by both tools]. ISOCIF has also a visualization tool and can transform the description of a magnetic structure to any setting, whereas STRCONVERT supports several file formats, including those of the ab initio code VASP (44), and is linked to MVISUALIZE (45) (also in the Bilbao Crystallographic Server) for direct visualization with Jmol (28).

2.3. *1k* Magnetic Structures and k-Maximal Magnetic Symmetries

Most of the reported commensurate magnetic structures are *1k* magnetic phases, i.e., their magnetic moment arrangements can be described as spin waves over the paramagnetic structure with a single independent propagation vector $\mathbf{k}$. The wave may be anharmonic, but the symmetry break is fully defined by the first harmonic of the frozen spin wave. *1k* magnetic configurations include the frequent case of magnetic orderings with $\mathbf{k} = 0$, in which the lattices of the magnetic and paramagnetic structures coincide. The propagation vector is directly accessible from diffraction experiments, and its value strongly restricts the possible magnetic symmetries. It is therefore very convenient to have tools that directly exploit this information. In general, the translation lattice of a *1k* magnetic ordering is given by those lattice translations $\mathbf{L}$ of the parent group $G1'$, such that $exp(i2\pi\mathbf{k}\cdot\mathbf{L}) = 1$. This condition defines a primitive supercell of a volume *n* times larger than that of the paramagnetic phase, with *n* being the minimal integer such that $n\mathbf{k}$ is a reciprocal lattice vector. In the case of *n* being even, those lattice translations of the paramagnetic phase that satisfy $exp(i2\pi\mathbf{k}\cdot\mathbf{L}) = -1$ are also preserved in the magnetic configuration but combined

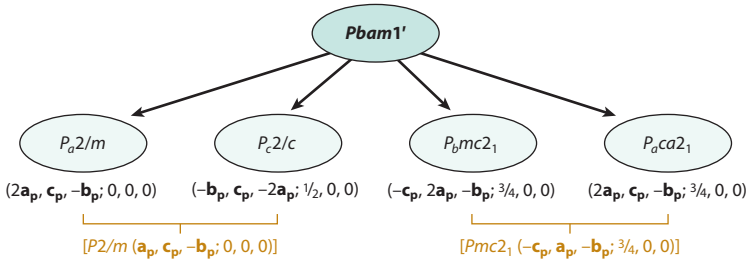

Figure 2

The four possible k-maximal magnetic symmetries for a magnetic ordering with propagation vector $\mathbf{k} = (1/2, 0, 0)$ on a paramagnetic phase with space group *Pbam*, as obtained with MAXMAGN. The transformation (from the parent *Pbam* basis) to the standard setting of each magnetic space group (MSG) is indicated. The index of the four subgroups is four. The corresponding effective space groups for the atomic positions (common to pairs of MSGs) are shown in gold.

with time reversal, i.e., they are maintained as antitranslations of type $\{1' \mid \mathbf{L}\}$. The resulting symmetry is therefore described by an MSG of type IV. When n is odd (including $\mathbf{k} = 0$), no antitranslations are possible, and the subgroup of $G1'$ describing the symmetry of the resulting structure is an MSG of type I or III.

The possible symmetries of a magnetic ordering with a propagation vector $\mathbf{k}$ are therefore limited to those compatible with the specific subgroup of lattice translations defined by $\mathbf{k}$ and, for even n, also with the additional set of antitranslations. This minimal symmetry is described by either the MSG $P1$ (lattice translations) for odd n or P_s1 for even n (lattice translations plus antitranslations). However, the propagation vector $\mathbf{k}$ is usually directed along special crystallographic directions, and larger subgroups of $G1'$ can be relevant. In general, a hierarchy of possible subgroups of $G1'$ consistent with the $\mathbf{k}$ vector is possible. Among this set of $\mathbf{k}$-consistent subgroups of $G1'$, those that do not have any supergroup fulfilling the same $\mathbf{k}$-consistency conditions are the possible maximal symmetry groups of the magnetic structure. We call them k-maximal subgroups or k-maximal magnetic symmetries for a given parent space group G and a given magnetic propagation vector $\mathbf{k}$. **Figure 2** depicts the k-maximal subgroups for *Pbam* and a magnetic propagation vector $\mathbf{k} = (1/2, 0, 0)$. This case is relevant for the magnetic structure of $GdMn_2O_5$ discussed above. Only four distinct types of magnetic ordering of k-maximal symmetry are possible, and one is in fact realized in $GdMn_2O_5$ (and other RMn_2O_5 compounds).

From general physical arguments (symmetry-dictated energy extrema at symmetrical configurations and smoothness of the energy landscape), one expects that magnetic orderings generally tend to keep as much symmetry as possible or, reversely, that the symmetry reduction tends to be minimal. Indeed, one can associate a k-maximal MSG with the majority of the known magnetic structures. The example in **Figure 2** is very illustrative, as it shows that two of the four possible maximal symmetries for the known propagation vector are polar (in both cases, along the *b* axis of the *Pbam* setting). Therefore, the derivation of the k-maximal MSGs allows one to infer directly that the system, if an insulator, is likely to be multiferroic. In fact, this is a quite general property of nonsymmorphic centrosymmetric space groups with cell-duplicating propagation vectors along the direction of one of the intrinsic nonprimitive translations of the nonsymmorphic operations. One can easily check with MAXMAGN (46) that this is sufficient for having noncentrosymmetric groups, polar in most cases, among the k-maximal symmetries.

k-maximal magnetic symmetry: magnetic symmetry group compatible with a given propagation vector having no supergroup also compatible

The number of k-maximal MSGs (a representative of each conjugacy class) is usually rather small, and each describes a possible, alternative, nonequivalent spin configuration. An efficient and

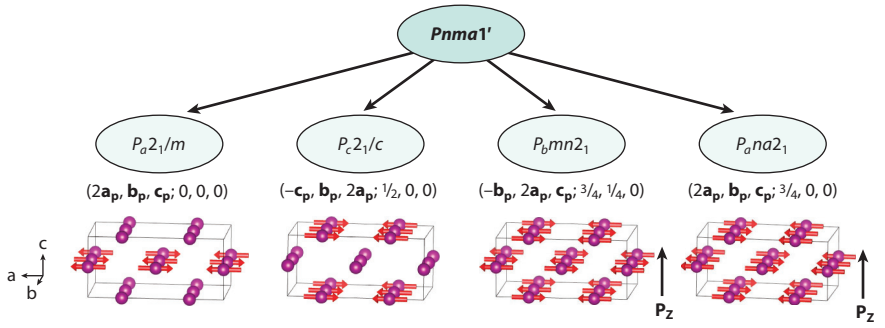

Figure 3

The four possible distinct magnetic orderings of maximal symmetry with propagation vector $\mathbf{k} = (1/2, 0, 0)$ for the Mn site in orthomanganites, as obtained with MAXMAGN, assuming that the spins are aligned along the *a* direction. The magnetic space group label associated with the magnetic symmetry of each structure is shown, together with the transformation (from the parent *Pnma*1′ basis) to its standard setting. The index of the four subgroups is four. The magnetic unit cell used in all figures is $(2\mathbf{a}_p, \mathbf{b}_p, \mathbf{c}_p; 0, 0, 0)$. The direction (with arbitrary sense) of the possible magnetically induced electric polarization P_z, when it is symmetry allowed, is indicated. The P_bmn2_1 ordering is the one observed in $HoMnO_3$ (22, 49). Abbreviation: P_z, possible magnetically induced electric polarization.

intuitive first step in the process of determining a magnetic structure with a known propagation vector is to enumerate and construct these alternative models of maximal symmetry for their subsequent contrast with experimental data or calculations. This first step can be done with the program MAXMAGN (46) in the Bilbao Crystallographic Server. This tool derives the k-maximal MSGs for any parent space group and any (reasonable) commensurate propagation vector. If the parent paramagnetic structure is introduced (in CIF format), it also produces the spin and structure models corresponding to each of the alternative k-maximal MSGs. These alternative models can be transported in magCIF format to refinement programs such as JANA2006 (47, 48) or FULLPROF (12) or to other computational tools for further analysis. These magCIF files can be visualized online with MVISUALIZE (45) or ISOCIF (41) or locally with VESTA (27) or Jmol (28).

As an example, **Figure 3** summarizes some of the results obtained for the case of $HoMnO_3$, a material with *Pnma* as the parent space group and propagation vector (1/2, 0, 0) (49). Of the four possible k-maximal symmetries, two are polar along *c*. Furthermore, the other two possible centrosymmetric monoclinic symmetries require that some of the Mn atoms remain with zero magnetic moment. Therefore, a full magnetic ordering of the Mn atoms with this propagation vector necessarily produces a symmetry breaking in which at least the *c* direction becomes polar. Thus, if the Mn atoms are fully ordered and the magneto-structural coupling is large enough, the material is bound to be a multiferroic with magnetically induced ferroelectricity (i.e., a type II multiferroic) (50). As in the preceding example, the index of the MSG is four, and there are two equivalent, nontrivial, twinned magnetic configurations related by inversion and with opposite electric polarizations.

2.4. Systematic Absences in the Magnetic Diffraction Diagram

MAGNEXT (34) can be used to derive the symmetry-forced systematic absences of magnetic, nonpolarized neutron diffraction for any MSG or MSSG. The presence of these systematic absences can sometimes help reduce the possible magnetic arrangements to be explored. Because MAGNEXT is directly accessed from MAXMAGN, the systematic absences for every alternative

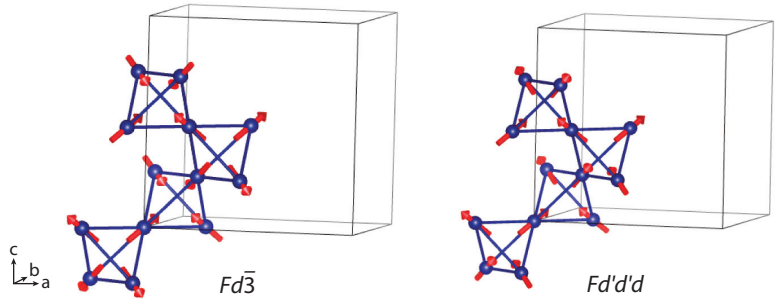

Figure 4

Scheme of the two possible magnetic models with zero propagation vector of maximal symmetry for the magnetic structure of $Na_3Co(CO_3)_2Cl$, as obtained with MAXMAGN. Only some Co atoms are depicted. These two maximal symmetries correspond to the so-called all-in/all-out and two-in/two-out models. Systematic absences in the diffraction pattern can distinguish the two models (see Section 2.4). The $Fd\bar{3}$ model is the one proposed in Reference 51 for this compound.

k-maximal magnetic symmetry can be consulted easily. Let us consider, for instance, the case of $Na_3Co(CO_3)_2Cl$ (51), which has a paramagnetic phase with space group $Fd\bar{3}$ (#203) and a magnetic phase with zero propagation vector. In this compound, the Co atoms at the 16*c* Wyckoff position form a highly frustrated pyrochlore-type framework. Using MAXMAGN, we can see that there are four k-maximal magnetic subgroups of $Fd\bar{3}1'$, but only two allow some nonzero spin for the Co atoms, namely $Fd\bar{3}$ (#203.26) and $Fd'd'd$ (#70.530) (the two subgroups are in their standard setting when using the parent unit cell). **Figure 4** shows a scheme of the spin arrangement for each of these two possible maximal symmetries. For $Fd\bar{3}$ the spin of the single independent Co at the origin must have the direction (1, 1, 1); in the alternative $Fd'd'd$ ordering, it can have any direction. When the (1, 1, 1) direction is also kept in this second arrangement, the two k-maximal symmetries basically correspond to spin orderings in the Co tetrahedra of the all-in/all-out and two-in/two-out types (**Figure 4**). These two alternative configurations are in fact often discussed as energetically favorable and have been observed in these pyrochlore-type materials. MAGNEXT shows that, in principle, they can be distinguished by the presence or lack in the magnetic diffraction of some systematic absences. For the subgroup $Fd\bar{3}$, all reflections of type (*h*, *h*, *h*) or (*h*, *0*, *0*) for any *h* value (and their cubic symmetry–related ones) are forbidden, whereas for the orthorhombic $Fd'd'd$ model, only magnetic reflections of type (*0*, *0*, *l*) are extinct. Twinning can, however, hamper the observation of these absences. In the case of the $Fd\bar{3}$ symmetry, the subgroup is of index two, and only a trivial twin with all spins reversed is possible, having no consequence in the diffraction diagram. But in the case of the $Fd'd'd$ structure, the subgroup index is six, and three nontrivial twinned configurations are expected to be superposed in the diffraction diagram, where the 3-fold rotation and its inverse could be taken as the twinning operations. The magnetic structure of $Na_3Co(CO_3)_2Cl$ reported in Reference 51 indeed possesses one of these two maximal symmetries, namely the MSG $Fd\bar{3}$ (22).

2.5. Hierarchy of Possible Magnetic Symmetries

If the models with k-maximal symmetry are not satisfactory to explain the experimental data, one can also use MAXMAGN to decrease the symmetry of the model in a controlled way. For this purpose, combining this program with the tool k-SUBGROUPSMAG (52) can be very helpful. This second program, also in the Bilbao Crystallographic Server, provides for any parent space group all possible magnetic symmetries consistent with one or more given propagation vectors,

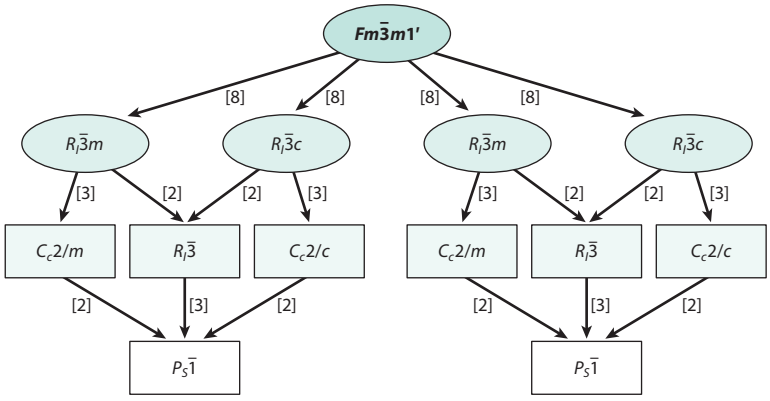

Figure 5

Graph obtained with k-SUBGROUPSMAG of all possible magnetic symmetries for a magnetic ordering with propagation vector (1/2, 1/2, 1/2) in a structure with space group $Fm\bar{3}m$. The subgroup index is indicated in brackets for each group-subgroup relation. The k-maximal magnetic space groups (MSGs) are highlighted with elliptical frames. Only one subgroup per conjugate class is shown, and the graph has been restricted to centrosymmetric subgroups. Subgroup labels only indicate the type and can be repeated. The MSG of NiO is one of the subgroups of type C_c2/c.

indicating their group-subgroup hierarchy. Let us consider, for instance, the magnetic structure of NiO (53). Its parent space group is $Fm\bar{3}m$ (#225) and its magnetic propagation vector is (1/2, 1/2, 1/2). **Figure 5** shows possible MSGs consistent with this propagation vector, as obtained with k-SUBGROUPSMAG. All k-maximal subgroups are in this case centrosymmetric, and for simplicity, we have limited the descending graph to their centrosymmetric subgroups. Some MSG labels are repeated, as some subgroups belonging to different conjugacy classes are MSGs of the same type. One can in fact distinguish two branches of subgroups with identical labels. The difference between them can be seen by comparing the operations of the minimal subgroup of type $P_s\bar{1}$ associated with each branch. In one of the branches, the inversion center at the origin is combined with time reversal, whereas in the other, it is not. The first branch is therefore not relevant for a full magnetic ordering of the Ni atoms, as the symmetry operation $\{-1' \mid 0, 0, 0\}$ would necessarily force a null spin for the Ni atom at the origin.

The magnetic structure of NiO (53) is depicted in **Figure 6**. Its symmetry is given by a monoclinic subgroup of type C_c2/c (*#15.90*) with the inversion center at the origin. Thus, it is not a k-maximal symmetry, and one has to go to a second level in the subgroup hierarchy depicted in **Figure 5** to obtain the relevant MSG. **Table 3** lists the operations of this subgroup, showing that the monoclinic axis is along the (1, −1, 0) direction. The index of this subgroup is 24. Therefore, 12 nontrivial twinned configurations can superpose in a single crystal diffraction diagram; 3 have the same propagation vector but have the monoclinic axis directed along the equivalent directions (1, −1, 0), (0, 1, −1), and (1, 0, −1), whereas the rest correspond to analogous configurations with rotated propagation vectors equivalent to (1/2, 1/2, 1/2). In the chosen setting, the Ni spins are reported to be within a good approximation directed along the (1, 1, −2) direction (53). One can check, however, with MAXMAGN that for this MSG, the Ni spins are only constrained to lie on the plane perpendicular to the monoclinic axis, having the general form (m_x, m_x, m_z). This is a less restrictive condition, and a weak spin component along the direction (1, 1, 1), which reduces the spin direction to its more general symmetry-allowed form has indeed been reported (53, 54). The symmetry of NiO is also compatible with a monoclinic distortion of the lattice [the effective

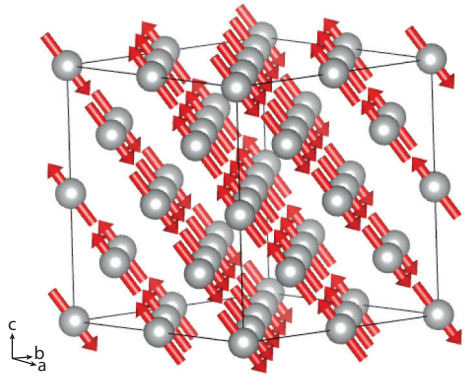

Figure 6

Magnetic structure of NiO (53) with indication of its magnetic space group. Only Ni atoms are shown.

space group *H* for the atomic positions is *C2/m* (#12)], but to our knowledge, no monoclinic strain has been observed. But in the case of CoO, which has a similar spin arrangement, such induced strain is known (55). Thus, the identification of the magnetic symmetry automatically indicates the possible phenomena that are the consequence of the symmetry reduction, although their magnitude may be too weak to be observable.

2.6. Multiple-*k* Magnetic Structures

Most of the reported magnetic structures have a single independent propagation vector. However, in the case of wave vectors related by the parent point-group symmetry (i.e., belonging to the same k-vector star), the experimental distinction between single-*k* or multiple-*k* structures is difficult to make. In many cases, the *1k* arrangement is taken as the simplest option, although multiple-*k* ordering could also explain the experimental data. Possible multiple-*k* spin arrangements can be explored in a systematic and symmetry-hierarchical form using k-SUBGROUPSMAG

Table 3 Operations that define the symmetry[a] of the magnetic phase of NiO[b]

N	(x, y, z)	Seitz notation
1	$x, y, z, +1$	$\{1 \mid 0, 0, 0\}$
2	$-y, -x, -z + 1/2, +1$	$\{2_{1-10} \mid 0, 0, 1/2\}$
3	$-x, -y, -z, +1$	$\{-1 \mid 0, 0, 0\}$
4	$y, x, z + 1/2, +1$	$\{m_{1-10} \mid 0, 0, 1/2\}$
5	$x, y, z + 1/2, -1$	$\{1' \mid 0, 0, 1/2\}$
6	$-y, -x, -z, -1$	$\{2'_{1-10} \mid 0, 0, 0\}$
7	$-x, -y, -z, -1$	$\{-1' \mid 0, 0, 1/2\}$
8	$y, x, z, -1$	$\{m'_{1-10} \mid 0, 0, 0\}$

[a]The magnetic space group type is C_c2/c in a nonstandard setting.

[b]The symmetry operations (modulo lattice translations) are given in the setting ($2\mathbf{a}_p$, $2\mathbf{b}_p$, $2\mathbf{c}_p$; 0, 0, 0), with $\mathbf{a}_p$, $\mathbf{b}_p$, $\mathbf{c}_p$ being the parent cubic basis. The cell ($2\mathbf{a}_p$, $2\mathbf{b}_p$, $2\mathbf{c}_p$) includes 16 centering translations generated by {1 | 1/4, 3/4, 0}, {1 | 1/4, 0, 3/4}, and {1 | 0, 1/4, 3/4}. The transformation to the standard setting of C_c2/c is indicated in **Figure 6**.

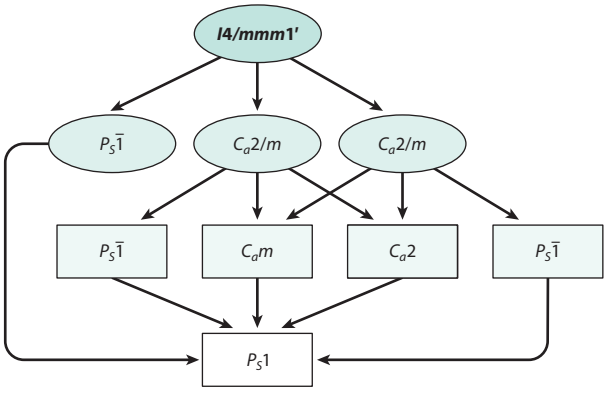

Figure 7

Graph (obtained with k-SUBGROUPSMAG) of all possible magnetic symmetries for a *2k* magnetic ordering with propagation vectors (−1/2, 0, 1/2) and (0, 1/2, 1/2) on a paramagnetic structure with space group *I4/mmm*. The k-maximal magnetic space groups are highlighted with elliptical frames. Only one subgroup per conjugacy class is shown. The magnetic ordering reported for $Sr_2F_2Fe_2OS_2$ (57) (see **Figure 8**) corresponds to one of the k-maximal subgroups of type C_a2/m.

combined with the tool MAGMODELIZE (56). The first program supplies all possible magnetic symmetries, together with their group-subgroup relations, for a given parent space group and a set of propagation vectors. Once one or several possible MSGs provided by k-SUBGROUPSMAG are chosen, the second program provides a model of the corresponding magnetic structures in magCIF format that can be tested and analyzed with other programs. As in the case of *1k* arrangements, the lattice is defined by the lattice translations **L** of the parent group *G1′* such that $exp(i2\pi\mathbf{k}_i \cdot \mathbf{L}) = 1$, for all the propagation vectors $\mathbf{k}_i$, whereas the set of translations (if any) satisfying $exp(i2\pi\boldsymbol{k}_i \cdot \mathbf{L}) = -1$ for all $\mathbf{k}_i$ are maintained in the possible magnetic groups as antitranslations $\{1' \mid \mathbf{L}\}$. k-SUBGROUPSMAG calculates all possible magnetic subgroups of the parent *G1′* having this lattice of translations and antitranslations (if they exist), and their group-subgroup hierarchy.

Figure 7 shows the graph obtained for a parent symmetry *I4/mmm*1′ and two wave vectors: $\mathbf{k}_1 = (-1/2, 0, 1/2)$ and $\mathbf{k}_2 = (0, 1/2, 1/2)$. This figure is relevant for $Sr_2F_2Fe_2OS_2$ (57), in which the magnetic ordering involves two of the wave vectors of the four-arms star of the point *N* in the Brillouin zone (58). The spin arrangement reported in Reference 57 is shown in **Figure 8**. Its symmetry is given by one of the k-maximal MSGs shown in **Figure 7**, namely the subgroup C_a2/m ($\mathbf{a}_p - \mathbf{b}_p - \mathbf{c}_p$, $2\mathbf{a}_p + 2\mathbf{b}_p$, $\mathbf{a}_p/2 - \mathbf{b}_p/2 + \mathbf{c}_p/2$; 0, 0, 0), demonstrating again the efficiency of looking for maximal compatible symmetry when searching probable spin orderings. A general magnetic structure complying with this MSG (or with any other subgroup of **Figure 7**) can be obtained in magCIF format using MAGMODELIZE (56). Although all other atoms split into two independent sites, the Fe site remains unsplit but becomes a general position, with its spin (and position) not constrained by symmetry. Thus, the aesthetically appealing tetragonal-like pattern of the model in **Figure 8*a*** is in fact not symmetry protected. Symmetry does not force an extreme of the energy map for this configuration. **Figure 8*b*** depicts a more general hypothetical arrangement with the same symmetry, showing the freedom existing in this phase, where the three spin components of the symmetry-independent Fe atom must in principle be determined.

2.7. Importance of Nonmagnetic Atoms

Magnetic atoms often occupy high-symmetry sites, and their spin arrangements are very simple, such that they can be described in simple terms without explicitly using an MSG or any specific

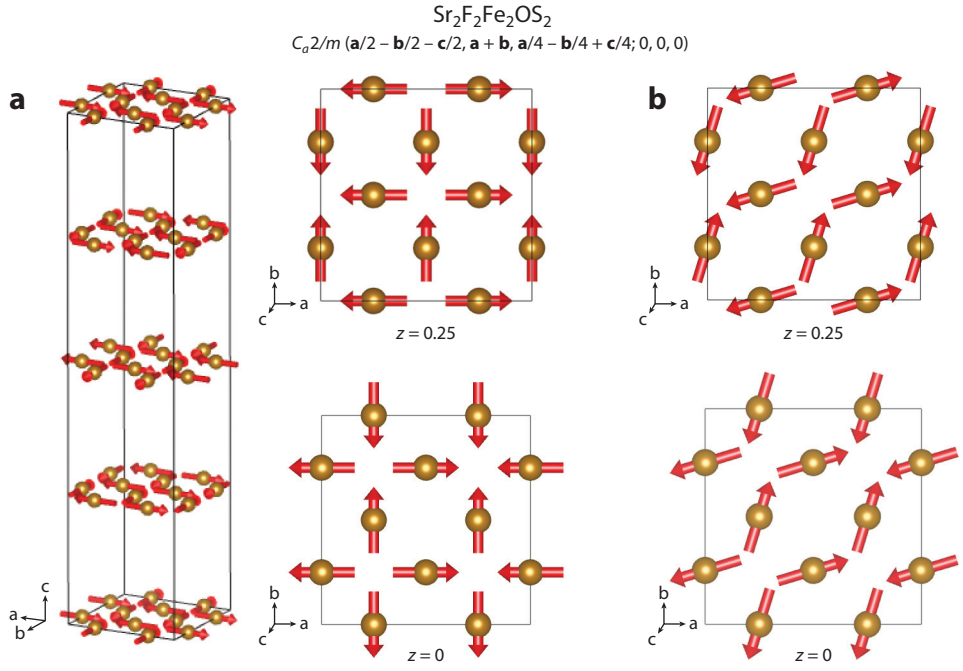

Figure 8

(*a*) 2*k* magnetic structure of $Sr_2F_2Fe_2OS_2$ (57) with a magnetic space group (MSG) of type C_a2/m (see **Figure 7**). The monoclinic axis is along the (1, 1, 0) direction. Only Ni atoms are shown. (*b*) Hypothetical structure with the same MSG as panel *a* showing the orientational freedom of the spins in this phase. A spin component along the *c* direction is also symmetry allowed.

symmetry consideration. However, to be able to predict and explain the properties of the resulting magnetic phase, one must be aware of the associated MSG, and this depends in general not only on the magnetic atoms but also on the actual positions of the nonmagnetic ones. Therefore, despite their irrelevance in magnetic diffraction, nonmagnetic atoms play an important role in the symmetry of a magnetic phase and its consequences.

Let us consider, for instance, the case of Gd_2CuO_4 (59). Its paramagnetic phase has been considered to have the space group *I4/mmm* (#139), with the magnetic Cu^{2+} occupying the Wyckoff position 2*a* (0, 0, 0). The reported magnetic ordering with propagation vector (1/2, 1/2, 0) is depicted in **Figure 9*a***. The magnetic symmetry of this simple spin arrangement of the body-centered Cu sublattice is given by the MSG C_Accm, again a k-maximal MSG for the observed propagation vector, and the collinearity of the spins along the (1, 1, 0) direction is symmetry protected. The magnetic point group of this MSG is *mmm*1′, i.e., a gray group, which forbids ferromagnetism. However, Gd_2CuO_4 is known to be a weak ferromagnet. This is due to the existence of a small structural distortion with the same wave vector (1/2, 1/2, 0) as the magnetic propagation vector, which decreases the effective parent space group symmetry from *I4/mmm* to *Cmce* (#64). This is sufficient to reduce the MSG to *Cm′ca′* (see **Figure 9*b***); the magnetic point group is then *m′mm′*, which allows a ferromagnetic component along the *b* direction of the standard setting, i.e., along the (1, −1, 0) direction in the tetragonal parent basis. The observed weak ferromagnetism is therefore a direct consequence of the orthorhombic structural distortion and is coupled with it. In terms of symmetry relations, the actual magnetic symmetry is the intersection of the subgroups

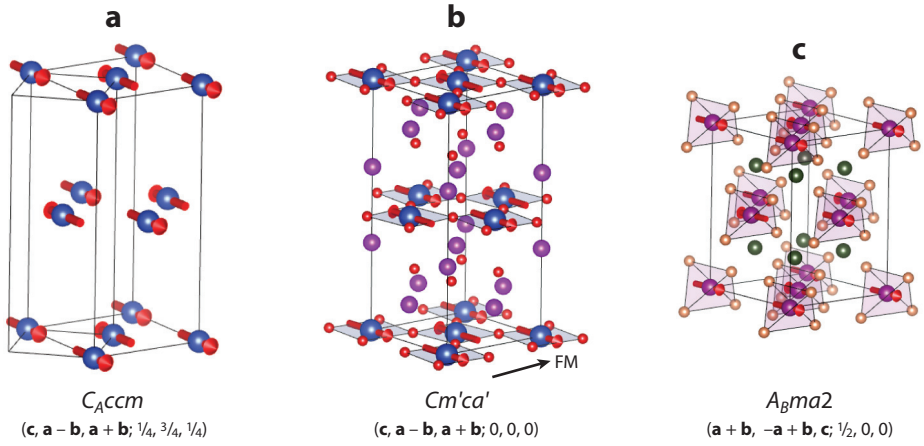

Figure 9

Simple spin arrangement in a body-centered tetragonal lattice of magnetic atoms, resulting in different symmetries and different magneto-structural properties depending on the parent space group of the structure as a whole: (*a*) $I4/mmm$, (*b*) $Cmce$, and (*c*) $I\bar{4}2m$. The transformation from the tetragonal basis to the standard setting of each magnetic space group (MSG) is given below each MSG label. The case in panel *b* with weak ferromagnetism is realized in Gd_2CuO_4 (59), and the case in panel *c* is a hypothetical multiferroic with a parent structure similar to the one of Ga_2MnSe_4 (63).

$Cmce1'$ and C_Accm, corresponding to the structural and magnetic distortions. But the resulting symmetry is also compatible with the presence of a ferromagnetic component that alone would yield another intermediate subgroup. A scheme of the group-subgroup relations corresponding to this symmetry breaking is depicted in **Figure 10**. This graph has the characteristic topology of three different symmetry-breaking distortions that are necessarily trilinearly coupled. Their switching is correlated by pairs, similar to what happens in other ferroic systems (60–62). Under some conditions, the two primary distortions can condense simultaneously in a single phase transition (61, 62).

The simple spin ordering of **Figure 9*a*** could also be sufficient to produce a polar phase if the symmetry of the paramagnetic phase considering all atoms were limited to $I\bar{4}2m$ (#121). **Figure 9*c***

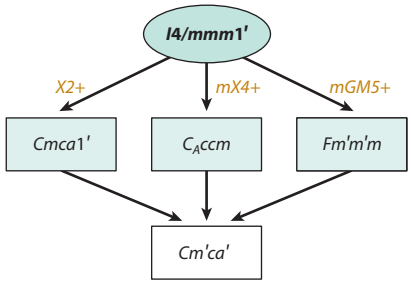

Figure 10

Scheme of the symmetry descent from the parent symmetry in the magnetic structure of Gd_2CuO_4 (59) showing the symmetry breakings of the primary structural and magnetic distortions and the triggering through symmetry compatibility of a ferromagnetic mode. The *irrep* labels of the distortions involved are indicated in gold (see Section 3). Notice that the group labels are the standard ones, and the orientations of their bases do not coincide.

shows the structure of Ga_2MnSe_4 (63), which has this parent space group, with a hypothetical spin ordering of the type in **Figure 9*a***. The MSG of this hypothetical phase would be A_Bma2 (#40.210). The magnetic point group is then reduced to $mm21'$, with the polar direction along the tetragonal axis. Thus, if the system were an insulator, this simple magnetic ordering could induce some ferroelectric polarization. These examples show the importance of identifying the magnetic symmetry, taking into account the nonmagnetic atoms, independently of the simplicity of the spin arrangement.

3. IRREDUCIBLE REPRESENTATIONS VERSUS MAGNETIC SPACE GROUPS

In accordance with Landau theory, a magnetic ordering very often defines an order parameter with transformation properties given by a single *irrep* of the parent symmetry. This is the basis of the representation method developed by Bertaut (6, 7), in which the possible magnetic orderings are parameterized with basis modes transforming according to *irreps* of the parent space group. The basis spin modes are restricted to a single *irrep* or, if necessary, to a set of *irreps*. Originally, the *irreps* were considered representations of an ordinary space group, but if one includes the transformation properties of the spin modes under time reversal, they are in fact *irreps* of the parent gray MSG, being odd for time reversal. To distinguish them from those that are even for time reversal (associated, for instance, with phonon modes), we call them magnetic *irreps* and include a prefix *m* in their label.

The relationship between the representation method and magnetic symmetry was initially the subject of an intense discussion (64–66), which provoked a kind of splitting between two communities and some unfortunate misunderstandings that have persisted for decades. Today, however, the program ISODISTORT (67) allows a comprehensive application of the two approaches. The use of this program permits one to characterize any magnetic ordering, commensurate or incommensurate, in terms of both magnetic symmetry and *irreps*, showing their generally complex relationship. Below, we briefly summarize this relation and some of the capabilities of ISODISTORT in this context.

In the simplest case that the active *irrep* is one-dimensional (1-D) and real, the spin arrangement will either change sign or be invariant when transformed by any of the operations of the gray space group. If an operation of the parent space group has the character -1 associated, the analogous operation combined with time reversal will necessarily have $+1$ associated, and all operations of the parent space group G will therefore be conserved, either pure or combined with time reversal. A one-to-one correspondence thus exists between the assignment of a 1-D *irrep* and an MSG. The *irrep* determines the MSG and vice versa, and the *irrep* basis spin modes define the same restrictions for the spin arrangement as those that can be directly derived from the MSG. However, this simple scenario is no longer true if the *irrep* is multidimensional. In this general case, different magnetic symmetries can occur for a single *irrep*. An arbitrary combination of the *irrep* basis modes results in a minimal symmetry given by the operations of the parent gray space group to which the *irrep* associates the identity matrix. This is the so-called kernel of the *irrep* (4, 68). But for specific combinations of the spin modes (i.e., specific directions in the space of the *irrep* or order parameter directions), higher magnetic groups called epikernels can be realized (68). Thus, the assignment of one MSG corresponding to an *irrep* epikernel introduces more constraints than the assignment of just the *irrep*, as it limits the possible combinations of the *irrep* basis modes. Epikernels and kernels are also called *isotropy* subgroups (67).

Traditionally, the representation method has been applied considering the full set of *irrep* basis modes; this implies that the symmetry of the configuration space being explored was therefore

generally the lowest one, i.e., the kernel of the *irrep*. Ad hoc restrictions in the basis modes introduced either a priori or as the result of the refinement could in fact make the spin model comply with one of the *irrep* epikernels, but in general, the representation method has been applied without monitoring or controlling the resulting symmetry. This scenario changes if ISODISTORT is used. This powerful program calculates the epikernels and kernel of any possible *irrep* and provides the corresponding models of the magnetic structure complying with each of these alternative symmetries in the form of a magCIF file. It can also supply a basis of spin modes consistent with each possible epikernel or with the kernel of an *irrep*. The program is very general and can also supply similar information if several *irreps* are active, deriving all possible alternative magnetic symmetries and corresponding models for a given set of *irreps*. Furthermore, it can be used in a reverse approach to decompose a given magnetic structure in terms of spin *irrep* modes, including structural *irrep* modes if some significant structural distortion with respect to the paramagnetic phase exists.

If the active *irrep* of a magnetic ordering is multidimensional, one can distinguish two different, rather common situations that we illustrate with example cases analyzed with ISODISTORT. The *irrep* labels used below are those of this program. The definitions and details of any of the *irreps* considered here can be examined with the tool REPRES (24) of the Bilbao Crystallographic Server, which uses the same notation.

Case 1: The symmetry of the magnetic structure is an *irrep* epikernel and a k-maximal MSG. In this case, the description of the magnetic structure using its MSG reduces the number of spin degrees of freedom with respect to the usual representation method. As an example, we can take the case of $GdMn_2O_5$ discussed in Section 2, with parent space group *Pbam* and propagation vector $\mathbf{k} = (1/2, 0, 0)$. There are two two-dimensional (2-D) *irreps* for this wave vector (point *X* in the Brillouin zone), labeled *mX1* and *mX2*, and **Table 4** lists their epikernels and kernels. Taking into account the equivalence of the transformations to standard setting, one can see that the four possible epikernels coincide with the four k-maximal MSGs discussed in Section 2. As shown in **Table 4**, the P_aca2_1 (#29.104) magnetic structure of $GdMn_2O_5$ discussed in Section 2 corresponds to a spin arrangement according to the *irrep mX2* but is restricted to a special direction within the *irrep* space that limits the number of degrees of freedom to 11, instead of the 22 that exist for a general *mX2* spin configuration. Similar to what can be done with MAXMAGN, once the *irrep* epikernel P_aca2_1 is chosen as the tentative symmetry of the structure, a magnetic structure model complying with this symmetry can be supplied by ISODISTORT

Table 4 Epikernels and kernels of the magnetic *irreps* of *Pbam*1′ at the point *X*[a]

Irrep	Order parameter direction	Magnetic space group	Transformation to standard	Number of spin degrees of freedom[b]
mX1	$(a, 0)$	P_bmc2_1 (#26.72)	$(\mathbf{c}_p, 2\mathbf{a}_p, \mathbf{b}_p; 1/4, 0, 0)$	2 (Gd), 5 (Mn)
	(a, a)	P_a2/m (#10.47)	$(-2\mathbf{a}_p, \mathbf{c}_p, \mathbf{b}_p; -1/2, 0, 0)$	2 (Gd), 5 (Mn)
	(a, b)	P_am (#6.21)	$(-2\mathbf{a}_p, \mathbf{c}_p, \mathbf{b}_p; 0, 0, 0)$	4 (Gd), 10 (Mn)
mX2	$(a, 0)$	P_aca2_1 (#29.104)	$(-2\mathbf{a}_p, \mathbf{c}_p, \mathbf{b}_p; -3/4, 0, 0)$	4 (Gd), 7 (Mn)
	(a, a)	P_c2/c (#13.72)	$(\mathbf{b}_p, \mathbf{c}_p, 2\mathbf{a}_p; 0, 0, 0)$	4 (Gd), 7 (Mn)
	(a, b)	P_cc (#7.28)	$(\mathbf{b}_p, \mathbf{c}_p, 2\mathbf{a}_p; 0, 0, 0)$	8 (Gd), 14 (Mn)

Abbreviation: *irrep*, irreducible representation.

[a]Epikernels and kernels that can be relevant for the magnetic ordering with a propagation vector (1/2, 0, 0) in $GdMn_2O_5$, as obtained with ISODISTORT.

[b]For the magnetic atoms in $GdMn_2O_5$.

in magCIF format and introduced for refinement in JANA2006 or FULLPROF. As explained in Section 2 (see **Table 2**), the 11 spin degrees of freedom of this structure are automatically taken into account in the crystallographic description of the magCIF file that makes use of the MSG. In such cases, the use of *irrep* modes brings no advantage or additional information in what concerns the magnetic degrees of freedom of the structure. Furthermore, we have seen in the previous section that all *irrep* epikernels in this example can be directly derived as k-maximal symmetries.

Case 2: The symmetry of the magnetic structure is an *irrep* epikernel but not a k-maximal MSG. In general, all k-maximal MSGs are *irrep* epikernels, but the reverse is not true for cubic, hexagonal, and trigonal parent symmetries, for which some *irrep* epikernels may not be k-maximal symmetries. In these cases, the magnetic symmetry given by the *irrep* epikernel allows, in general, spin degrees of freedom corresponding to other *irreps*. The most efficient approach in such situations is to decompose the spin degrees of freedom into *irrep* spin modes that should be restricted or symmetry-adapted to the relevant MSG.

The magnetic structure of NiO discussed above is a simple example of this situation. There is only a single Ni atom per primitive unit cell, and therefore the *irrep* spin modes are defined by the spin of this single site. The magnetic representation of the Ni moments with propagation vector (1/2, 1/2, 1/2) (point *L* in the Brillouin zone) decomposes into *mL2*+ ⊕ *mL3*+. The small *irreps* corresponding to *mL2*+ and *mL3*+, relevant for *1k* spin arrangements, are 1-D and 2-D, respectively. Thus, the three spin degrees of freedom of the system decompose into a single spin mode of type *mL2*+ and two spin modes for the *irrep mL3*+. **Table 5** shows that a magnetic model according to the *irrep mL2*+ is equivalent to the assignment of the MSG $R_I\bar{3}c$ (#167.108), which is one of the k-maximal MSGs shown in **Figure 5**. Under this symmetry, the Ni moment is constrained along the (1, 1, 1) direction, i.e., the *mL2*+ spin Ni mode is just a spin directed along the (1, 1, 1) direction; this can be checked by applying the usual programs used in the representation method [BASIREPS (12), SARA*h* (13), or MODY (14)]. For the 2-D small *irrep mL3*+, the situation is quite different. The mentioned programs provide two basis spin modes for *mL3*+, and if both are used, the explored magnetic configurations have the lowest possible symmetry, namely the *irrep* kernel $P_S\bar{1}$. The Ni spin is then only restricted to lie on the plane perpendicular to the (1, 1, 1) direction. In order to restrict the *irrep* model to one of the

Table 5 Epikernels and kernels of some magnetic *irreps* of $Fm\bar{3}m1'$ at the *L* point[a] of the Brillouin zone

Irrep	Order parameter direction	Magnetic space group	Transformation to standard	Spin degrees of freedom[b]	Ni spin basis modes
mL2+	(*a*)	$R_I\bar{3}c$ (#167.108)	$(-\mathbf{a}_p/2 + \mathbf{c}_p/2, \mathbf{b}_p/2 - \mathbf{c}_p/2, -2\mathbf{a}_p - 2\mathbf{b}_p - 2\mathbf{c}_p; 0, 0, 0)$	1	(1, 1, 1)
mL3+	(*a*, 0)	C_c2/m (#12.63)	$(\mathbf{a}_p/2 + \mathbf{b}_p/2 - \mathbf{c}, \mathbf{a}_p/2 - \mathbf{b}_p/2, -\mathbf{a}_p - \mathbf{b}_p; 0, 0, 0)$	1	(1, −1, 0)
	(*a*, *a*)	C_c2/c (#15.90)	$(\mathbf{a}_p/2 + \mathbf{b}_p/2 - \mathbf{c}, \mathbf{a}_p/2 - \mathbf{b}_p/2, -\mathbf{a}_p - \mathbf{b}_p; 0, 0, 0)$	1	(1, 1, −2)
	(*a*, *b*)	$P_S\bar{1}$ (#7.28)	$(-\mathbf{b}_p/2 + \mathbf{c}_p/2, \mathbf{a}_p/2 - \mathbf{b}_p/2, \mathbf{a}_p + \mathbf{c}_p; 0, 0, 0)$	2	(1, −1, 0) (1, 1, −2)

Abbreviation: *irrep*, irreducible representation.

[a]Epikernels and kernels that can be relevant in the magnetic phase of NiO with propagation vector (1/2, 1/2, 1/2), as obtained with ISODISTORT (only *1k* configurations are included).

[b]For the Ni atoms.

epikernels, one must choose a specific linear combination of the two basis modes of *mL3+*. These epikernel-adapted modes can be obtained with ISODISTORT and are listed in **Table 5**. The MSG of the magnetic structure of NiO is C_c2/c (#15.90). Therefore, the active *irrep* is *mL3+* but is restricted to one of its epikernels, with the spin mode being along the (1, 1, −2) direction. We saw in the previous section, however, that the C_c2/c symmetry only restricts the Ni spin to lie on a plane of the form (m_x, m_x, m_z). This symmetry therefore also allows an orthogonal spin component along the (1, 1, 1) direction.

Hence, the symmetry assignment of the MSG C_c2/c (#15.90) restricts the spin configuration with respect to a general *mL3+* arrangement, but, at the same time, it allows the presence of a mode according to the *irrep mL2+*. The reason for the possible presence of this secondary spin mode can be seen in **Figure 5**. C_c2/c is not a k-maximal symmetry but is in fact a subgroup of the epikernel of *mL2+*. Therefore, in accordance with von Neumann principle, the symmetry break produced by the primary *mL3+* order parameter allows the presence of an *mL2+* distortion as a symmetry-compatible secondary effect. Thus, the MSG automatically takes into account all degrees of freedom that are triggered by the symmetry break. From physical arguments, one should expect that the prevailing spin direction will comply with the *mL3+ irrep* but will be restricted to the relevant epikernel and will therefore be along the (1, 1, −2) direction, whereas the *mL2+* component along the (1, 1, 1) direction should be weak or even negligible. This is indeed what is observed.

Therefore, the most efficient approach in this type of case is to consider both the magnetic symmetry of the system represented by an MSG and the decomposition of the degrees of freedom in terms of *irrep* modes restricted to this MSG. In general, a physical hierarchy between the symmetry-compatible *irreps* will exist, and the degrees of freedom associated with the secondary *irreps* may be disregarded, reducing their number with respect to a description using only the MSG.

A more complex example is summarized in **Figure 11**, which shows all the possible $\mathbf{k} = 0$ magnetic symmetries for the compound $Na_3Co(CO_3)_2Cl$, discussed in Section 2.4. The figure also indicates the possible *irrep* epikernels and kernels and the number of *irrep* basis modes in each case. For instance, a general spin configuration according to the *irrep mGM4+* requires nine basis modes, and its magnetic symmetry is the minimal one, $P\bar{1}$, but it allows three additional degrees of freedom corresponding to the secondary symmetry-compatible *irreps mGM1+* and *mGM2+* ⊕ *GM3+* (a physically irreducible *irrep*). But the *irrep mGM4+* can also yield the MSG $R\bar{3}$ (#148.17), and under this symmetry, the number of free spin parameters is four. But this MSG restricted to the *irrep mGM4+* only requires three basis modes, whereas the fourth degree of freedom corresponds to the symmetry-compatible mode for the *irrep mGM1+* of symmetry $Fd\bar{3}$ (#203.26).

4. INCOMMENSURATE MAGNETIC STRUCTURES AND SUPERSPACE SYMMETRY

4.1. Magnetic Superspace Groups

The superspace symmetry formalism, developed between 1974 and 1985, has become the standard method for the analysis and determination of nonmagnetic modulated structures, both incommensurate and commensurate (5, 69–74). Nearly all quantitative structural studies of these systems employ the refinement program JANA2006 (47, 48), which is based on this formalism. A superspace group defines all the structural constraints that are symmetry forced and are protected within an incommensurate phase, playing the role that an ordinary space group does for commensurate phases. Since the beginning of its development, it was pointed out that superspace symmetry can be extended to magnetic systems (5), but in fact only a few testimonial works have

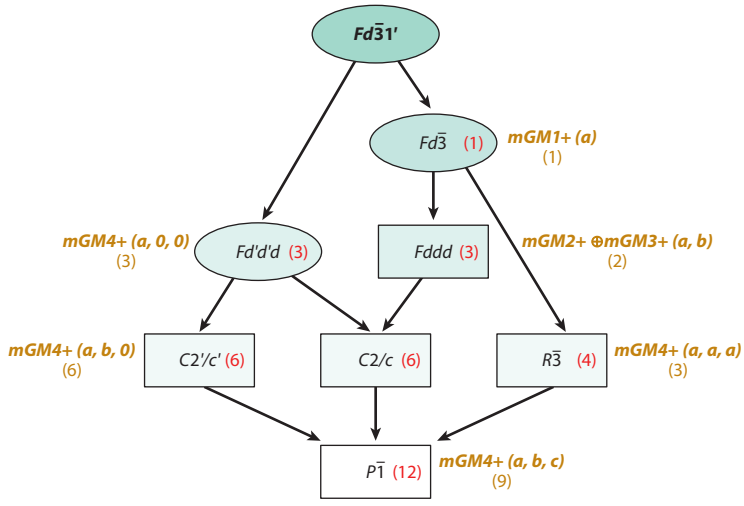

Figure 11

Group-subgroup graph of all possible magnetic symmetries for a structure with parent space group $Fd\bar{3}$ (#203), propagation vector zero, and a magnetic atom at the origin. The k-maximal magnetic space groups are highlighted with elliptical frames. Only one subgroup per conjugacy class is shown. The subgroups that are epikernels for some irreducible representations (*irreps*) have at their side the corresponding *irrep* label with the order parameter direction in the ISODISTORT notation. The number of spin degrees of freedom is indicated in red for each group, and the number of symmetry-restricted *irrep* basis modes is written in gold below the *irrep*.

applied this formalism to magnetic structures (75). The situation has drastically changed in the past few years with the development of computational tools specific for magnetic structures that make use of superspace symmetry, in particular the extension of JANA2006. Hence, the number of reported incommensurate magnetic structures refined, described, or both using superspace symmetry is increasing steadily (76–87). For the sake of simplicity, we restrict the discussion to *1k* incommensurate structures but we stress that superspace symmetry can also be considered in more general cases with several independent, incommensurate wave vectors.

In practical terms, the characterization of a *1k* incommensurate phase using a superspace group is reduced to the description of the local aperiodic atomic positions and atomic properties (as the magnetic moments) by means of periodic modulation functions of a continuous variable, say x_4, with period 1. The actual value of an atomic property of an atom at a position $\mathbf{r}$ is then given by the value of the corresponding modulation function at $x_4 = \mathbf{k} \cdot \mathbf{r}$. The continuous variable of these functions is associated with the additional dimension in a mathematical superspace, which is introduced in the definition of the symmetry operations. A symmetry operation of an incommensurate structure is, in general, an ordinary symmetry operation of the reference parent structure, say, $\{\mathbf{R} \mid \mathbf{t}\}$ followed by a certain global shift τ of all the modulation functions, such that the transformed system with the atomic positions and local properties given by these shifted modulation functions becomes undistinguishable from the original one. The operation is then represented by $\{\mathbf{R} \mid \mathbf{t}, \tau_0\}$, with $\tau_0 = \tau + \mathbf{k} \cdot \mathbf{t}$ being the k-independent part of the phase shift. Thus, the symmetry group of an incommensurate crystal is obtained by adding the possibility of shifting the global phase of all the modulation functions to the ordinary rotations, roto-inversions, and translations. A generalization to magnetic crystals is immediate by just including among the possible operations the combination with time reversal, yielding the MSSGs. As ordinary magnetic symmetry, MSSGs are robust in the

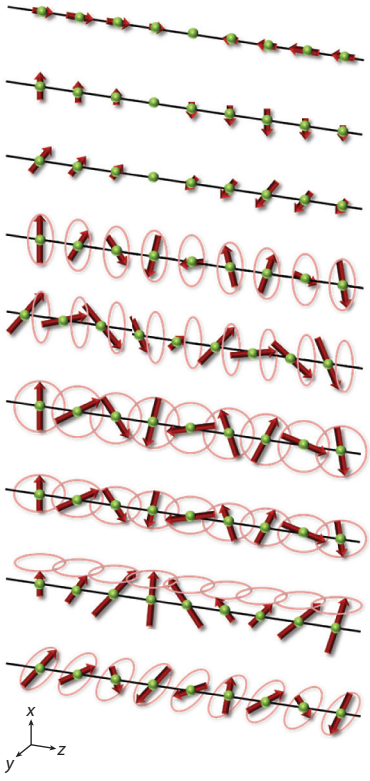

	Point group		
	No lattice	Cubic lattice	Hexagonal lattice
Collinear longitudinal	$\infty/mm1'$	$4/mmm1'$	$6/mmm1'$
Collinear transversal	$mmm1'$	$mmm1'$	$mmm1'$
Collinear transversal oblique	$12/m11'$	$12/m11'$	$12/m11'$
Proper screw	$\infty21'$	$4221'$	$6221'$
Conical screw	$\infty2'$	$42'2'$	$62'2'$
Cycloid	$2mm1'$	$2mm1'$	$2mm1'$
Elliptical cycloid	$2mm1'$	$2mm1'$	$2mm1'$
Transverse cone	$2'mm'$	$2'mm'$	$2'mm'$
Elliptical oblique cycloid	$1m11'$	$1m11'$	$1m11'$

Figure 12

Representative spin modulations along a periodic chain of atoms with indication of their point-group symmetries according to their superspace symmetry groups. The first column is the point group of a single chain, whereas the second and third columns list those for three-dimensional cubic and hexagonal monoatomic arrangements of these chains, the chains being along the *c* direction.

sense that they can be associated with the properties of the system within a whole thermodynamic phase. The point-group symmetry constraining the tensor physical properties of the phase is then formed by the point-group operations that form part of the symmetry operations of the MSSG.

Following the basic principles explained above, deriving the magnetic point-group symmetry of a chain of spins with an incommensurate modulation of any type is straightforward. **Figure 12** shows the point-group symmetries of the most representative incommensurate spin modulations along a periodic atomic chain. In nearly all cases, the point group is gray, i.e., it contains time reversal, and linear magneto-structural couplings are therefore not possible. Only those spin modulations that include a $\mathbf{k} = 0$ component in addition to the incommensurate frozen spin wave have nongray point groups. This is a general property: Any *1k* incommensurate modulation possesses the superspace symmetry operation $\{1' \mid 0, 0, 0, 1/2\}$ because, after switching the spins to opposite signs by the action of time reversal, a phase shift of 1/2 of the spin modulation as a whole recuperates the original spin arrangement.

Many of the point groups of the incommensurate spin chains in **Figure 12** include inversion, or other operations transforming $\mathbf{k}$ into $-\mathbf{k}$. Only the cycloid arrangements and the transverse

conical modulation break the symmetry into noncentrosymmetric polar groups. The polarity of a circular spin cycloid is along the direction perpendicular to **k** and within the plane of the cycloid. Thus, symmetry is sufficient to predict the polar character (and its direction) for this type of spin arrangement. Notice, however, that in the case of an elliptical oblique cycloid, with the main axes of the cycloid ellipse along arbitrary directions, the symmetry is reduced to $m1'$, with the mirror plane being the one of the cycloid. Hence, in this case, the possible induced polarization can take an arbitrary direction within this plane.

It is important to stress that a proper screw modulation, with the spins rotating on the plane perpendicular to the propagation vector, also breaks inversion but keeps any binary axis perpendicular to the chain. Thus, this type of spin arrangement in high-symmetry lattices gives way to a noncentrosymmetric but nonpolar chiral symmetry. This is, for instance, the case of $MnAu_2$ (22, 88), with space group *I*4/*mmm* (#139) in the paramagnetic phase and MSSG $I4221'(00\gamma)q00s$ (point group 4221′) in its incommensurate magnetic phase. However, if these types of screw spin chains are embedded in a structure lacking binary axes perpendicular to the direction of the modulation, the magnetic symmetry will be polar along the chain, and in the case of an insulator, an induced ferroelectric polarization along the direction of the propagation vector is possible.

4.2. Crystallographic Description of Incommensurate Magnetic Structures

A CIF dictionary for incommensurate (nonmagnetic) structures based on superspace symmetry already exists (89), and its extension to magnetic structures within the magCIF dictionary is straightforward. In the simplest case of a harmonic modulation, the spin modulation functions of a magnetic atom in the asymmetric unit are given by a combination of sine and cosine functions for each spin component. If the site lies in a special position, then the modulation is subject to site-symmetry constraints, whereas the spin modulation functions of the symmetry-related atoms are derived by the operations of the superspace group. A detailed review of the application of MSSGs in magnetic structures can be found in Reference 3.

As an example, we consider the very simple structure of Ce_2Pd_2Sn (90, 91), shown in **Figure 13**. This is a sinusoidal transversal spin modulation, of the Ce magnetic moments along *c*, with parent space group *P*4/*mbm* (#127) and propagation vector $\mathbf{k} = (0.105, 0, 0)$. The superspace symmetry of this spin arrangement is given by the MSSG $Pbam1'(\alpha 00)0s0s$ (22), maintaining the parent setting for the average structure. This means that the structure is centrosymmetric, and its average symmetry is reduced from tetragonal to $Pbam1'$, which implies the possible liberation of structural degrees of freedom with respect to the parent phase through magneto-structural coupling. The 4*h* Ce site in the parent tetragonal phase remains a 4*h* site in the $Pbam1'$ average structure, and only the spin modulation of one atom, Ce1, is independent. The representative operations of $Pbam1'(\alpha 00)0s0s$ are $\{2_{100} \mid 1/2, 1/2, 0, 1/2\}$, $\{2_{010} \mid 1/2, 1/2, 0, 1/2\}$, $\{2_{001} \mid 0, 0, 0, 0\}$, $\{-1 \mid 0, 0,$

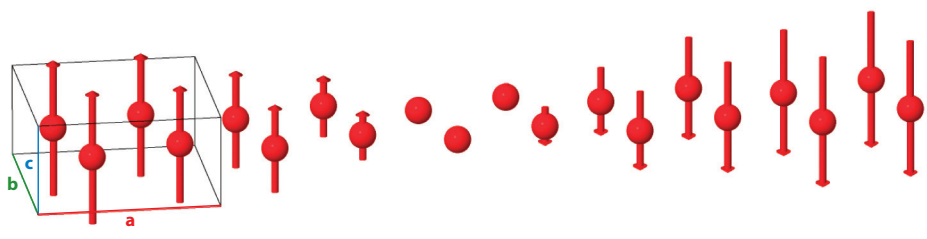

Figure 13

Incommensurate magnetic structure of Ce_2Pd_2Sn (54) with superspace group $Pbam1'(\alpha 00)0s0s$.

0, 0}, {m_{100} | 1/2, 1/2, 0, 1/2}, {m_{010} | 1/2, 1/2, 0, 1/2}, and {m_{001} | 0, 0, 0, 0}, plus those obtained by combining all these operations with {1′ | 0, 0, 0, 1/2} (22). The symmetry invariance of the Ce1 site for the operation {m_{001} | 0, 0, 1, 0} constrains its spin modulation to be along the *c* direction:

$$\vec{M}_{Ce1}(x_4) = (0, 0, M_{z\cos 1})\cos(x_4) + (0, 0, M_{z\sin 1})\sin(x_4).$$

The spin modulation therefore has two free parameters. The modulation functions of the other three Ce atoms in the parent unit cell, Ce1_2, Ce1_3, and Ce1_4, are obtained through the operations {m_{010} | 1/2, 1/2, 0, 1/2}, {m_{100} | 1/2, 1/2, 0, 1/2}, and {−1 | 0, 0, 0, 0}, respectively (see Reference 3). Hence, Ce1_2 has the same modulation function as Ce1_1, whereas the other two atoms have the same cosine term but an opposite sine component. This implies that symmetry allows a phase shift between the modulations of the Ce atoms that are related by operations transforming **k** into −**k** but constrains all amplitudes to be equal. According to the model reported in References 90 and 91, the parameter $M_{z\sin 1}$ is negligible, and the four modulations are in phase.

4.3. Irreducible Representations Versus Magnetic Superspace Groups

The relationship of the representation approach with the MSSGs is similar to the one discussed above between *irreps* and MSGs in commensurate structures (3). If the small *irrep* associated with the spin modulation is 1-D, there is a one-to-one correspondence between the MSSG and the *irrep*, but for multidimensional small *irreps* in general, several distinct MSSGs can be realized in the incommensurate phase depending on the direction taken by the order parameter within the representation space. Hence, different magnetic symmetries can result from the same *irrep*, constituting the epikernels and kernel of the *irrep*.

However, an important difference exists with respect to the commensurate case. For 1-D small *irreps*, even if only one MSSG is possible, this MSSG generally includes operations that transform the vector **k** into −**k** (if these operations exist in the paramagnetic phase). **Figure 14** shows the four MSSGs corresponding to the four possible *irreps* of *P*4/*mbm* for an incommensurate wave vector (α, 0, 0), which could be relevant for the case of Ce_2Pd_2Sn described above. All are centrosymmetric. Among the wave vector's superspace symmetry operations, the MSSGs keep all point-group operations of the parent symmetry that either maintain **k** invariant or transform it to −**k**. This is an important difference from the traditional representation approach, which has usually considered that atoms related by operations of the parent symmetry that transform **k** into −**k** become split in the incommensurate phase, yielding independent suborbits of atoms. In practice, some correlations between the parameters of these supposedly independent atoms are often introduced and justified with various arguments not related to symmetry. However, this example shows that, according to the MSSG associated with any active *irrep*, the modulations of atoms related by these −**k** operations remain symmetry related in the incommensurate phase. The spin arrangement of Ce_2Pd_2Sn complies with the *irrep mDT4* (see **Figure 14**), and the representation method yields three free parameters for this *irrep* (91) (one amplitude and phase per suborbit of Ce atoms, minus one free phase that can be fixed arbitrarily). Thus, in principle the method allows different amplitudes of the spin modulations of the two suborbits, although in practice they are made equal (91). The MSSG associated with the *irrep* shows that this is not just an additional reasonable assumption or approximation but is part of the restrictions for a single *irrep* distortion, i.e., a single order parameter. One can always derive them from the *irrep* transformation properties, as done in Reference 92, for instance, but the identification of the MSSG associated with the active *irrep* provides automatically all constraints, including those of possible higher modulation harmonics, both magnetic and structural. The usual disregard of the symmetry constraints coming from the operations changing **k** into −**k** implies that more

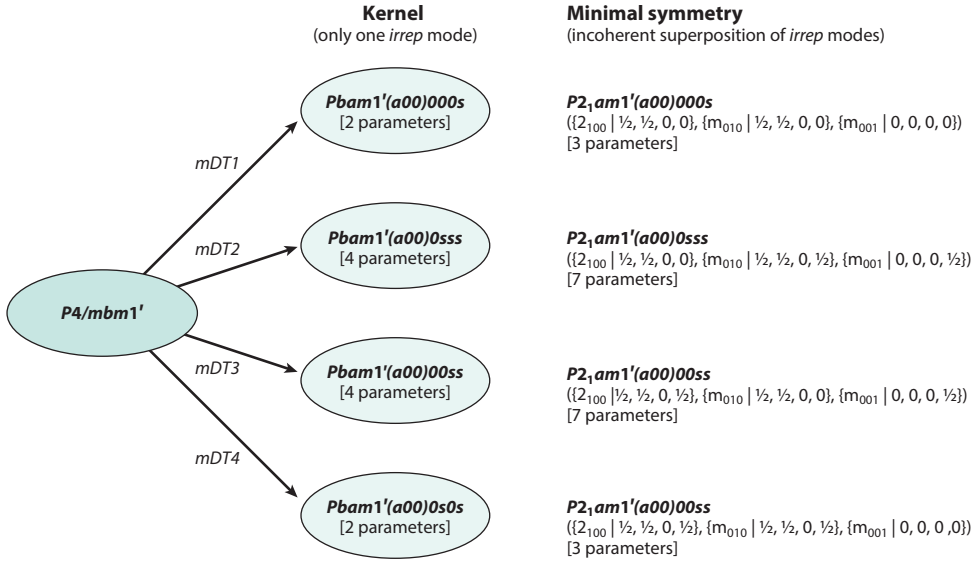

Figure 14

Possible magnetic superspace groups for an incommensurate magnetic modulation with propagation vector of type (α, 0, 0) on a parent structure with space group *P4/mbm*, if restricted to a single irreducible representation (*irrep*) mode, as can be obtained in JANA2006 or ISODISTORT. The number of free magnetic parameters for each case is indicated in brackets. A set of generators is listed for each symmetry, with the exception of $\{-1 \mid 0, 0, 0, 0\}$ and $\{1' \mid 0, 0, 0, 1/2\}$, present in all. The minimal superspace symmetry, corresponding to an incoherent superposition of more than one *irrep* mode, is shown on the right. Notice that the superspace groups are described here in the parent setting, in contrast with the default output of ISODISTORT.

general spin arrangements are being considered, which represent the incoherent (phase-shifted) superposition of more than one *irrep* mode for the same *irrep*. Notice, for instance, that in the case of Ce_2Pd_2Sn, the constraint coming from the **k** to −**k** transforming operations is essential to keep the system centrosymmetric.

ISODISTORT or JANA2006 provide the epikernels and kernel of any incommensurate *irrep* in the form of a list of possible MSSGs, and they can supply the corresponding symmetry-adapted magnetic structure models for visualization or any further analysis. The models are portable using incommensurate magCIF files, which are fully supported by the visualization program Jmol. JANA2006 can in principle refine any incommensurate *1k* magnetic structure under any chosen MSSG, and the program includes the calculation tool of epikernels and kernels for the possible *irreps* as a preliminary step to explore and construct all possible models of different superspace symmetry that can be confronted with the experimental data. Once one *irrep* epikernel (or kernel) is chosen, the program works in a crystallographic way using the corresponding MSSG to analyze the symmetry of the diffraction data and constrain both magnetic and structural parameters. This allows a systematic search of the incommensurate magnetic structure in a symmetry-hierarchical way. It works by default in the parent setting, but it can be changed by the user. By contrast, ISODISTORT supplies the different possible MSSG models in their standard setting, which can strongly differ from the one of the parent phase, including a different choice of the propagation vector. This program focuses on the mode analysis of both the magnetic and structural degrees of freedom of the different possible phases and supplies a parameterization in terms of *irrep* basis

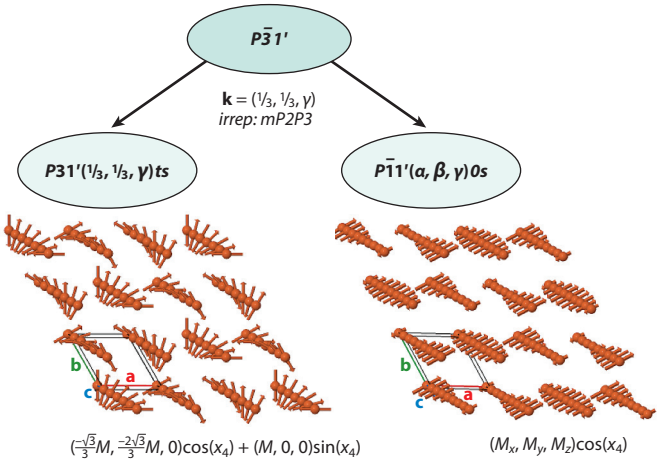

Figure 15

Epikernels of the irreducible representation (*irrep*) *mP2P3* (physically irreducible) with a propagation vector of type (1/3, 1/3, γ) for a parent space group $P\bar{3}$ (#147) and corresponding spin arrangements for an atom at the origin, as obtained from JANA2006 or ISODISTORT. The general form of the spin modulation is also indicated for each case. These two alternative k-maximal symmetries are realized in the phase diagram of $RbFe(MoO_4)_2$ (82, 93).

modes adapted to the relevant MSSG. This is very important when several *irreps* are symmetry allowed, as one can distinguish primary *irrep* modes from weak or negligible secondary ones.

Figure 15 summarizes the case of $RbFe(MoO_4)_2$ (82, 93). This compound has a paramagnetic phase with space group $P\bar{3}$, and it orders with an incommensurate propagation vector (1/3, 1/3, γ) [line *P* in the Brillouin zone (58)]. Having the Fe atom at the origin, a spin arrangement with this propagation vector in the most general case would require five parameters (the amplitude and phase for the three spin components, minus one phase that can be chosen arbitrarily). However, the modulation of the spin component along *c* transforms according to the *irrep mP1*, whereas those on the *ab* plane correspond to the *irrep mP2P3* (a physically irreducible *irrep*). The *irrep mP2P3* has two possible epikernels. This means that two different alternative MSSGs of maximal symmetry are possible for this *irrep*. Their labels are indicated in **Figure 15**, together with the mathematical form of the spin modulation function and a graphical scheme. The system can either maintain the 3-fold axis and lose the space inversion symmetry or keep the centrosymmetry but break the 3-fold axis. In the first case, the MSSG forces the spin modulation to have two orthogonal components in quadrature on the *ab* plane; this is sufficient to acquire a typical 120° arrangement on the *ab* plane, whereas the spins rotate along *c*, forming a screw with a pitch determined by the propagation vector. If this MSSG is assigned, the determination of the corresponding spin configuration requires a single parameter. A magnetic phase with this superspace symmetry has 31′ as point-group symmetry. It is therefore polar along *c*, with domains related by the lost space inversion. Induced ferroelectricity, i.e., a multiferroic of type II, should be expected (93).

The other alternative maximal symmetry is a collinear arrangement in which the modulations of the three moment components are in phase. This second MSSG has three free spin parameters, but one of them is the M_z component (see **Figure 15**), which corresponds to the *irrep mP1*. As in the commensurate case, the magnetic symmetry allows degrees of freedom corresponding to symmetry-compatible secondary modes associated with *irreps* having as epikernel (or kernel) one supergroup of the actual MSSG. This is the case of the M_z modulation that can be present, as a secondary *mP1* distortion, in a model complying with this MSSG $P\bar{1}1'(\alpha, \beta, \gamma)0s$, provided it is

in phase with the primary *mP2P3* collinear distortion on the *ab* plane. This second component can be small enough to be negligible, reducing the number of free parameters to two. Notice that for this MSSG, the *x* and *y* components of the propagation vector are no longer forced to have the rational value 1/3, as explicitly indicated in the group label. This second alternative maximal superspace symmetry is realized in the phase diagram under magnetic field.

The kernel of *mP2P3*, i.e., the lowest superspace symmetry possible, is the intersection of the two alternative k-maximal superspace symmetries for *mP2P3* discussed above. It reduces to the

Table 6 Databases and programs to analyze magnetic structures using magnetic symmetry[a]

Program or database	Program description
Magnetic group tables (30)	Tables of MSGs with illustrations and data analogous to those of the ordinary space groups in the *International Tables for Crystallography*. They are set in OG notation and are not computer readable.
ISO-MAG (33)	Computer-readable tables and data of MSGs in both BNS and OG notations.
MGENPOS, MWYCKPOS (34)	Database of symmetry operations and Wyckoff positions of MSGs in both BNS and OG notations.
IDENTIFY MAGNETIC GROUP (39)	Identifies a magnetic space group (commensurate) from a set of generators in an arbitrary setting.
ISOCIF (41), FINDSYM (43)	Editor to create or modify a magCIF file of a commensurate magnetic structure. It transforms to any desired setting and automatically finds the actual MSG of a structure introduced enumerating all atoms and spins in the unit cell. It includes an online visualization tool.
STRCONVERT (42)	Editor to convert, edit, or both a commensurate magnetic structure into different file formats, including magCIF. Using FINDSYM, it finds the MSG of the structure if transformed or given in *P*1 symmetry. VASP files for or from ab initio calculations are also supported.
ISODISTORT (67)	Comprehensive online program to enumerate and describe possible magnetic structures caused by one or more active *irreps*. The magCIF format is supported. It provides possible epikernels and kernels (isotropy subgroups) of any magnetic *irrep* or set of *irreps* and can yield the mode decomposition of any commensurate magnetic structure if given in magCIF format. Standard settings are required for input data, but the resulting models of the magnetic structures can be obtained in any chosen setting.
MAXMAGN (46)	Generates all possible magnetic symmetries and the corresponding magnetic structures for a given propagation vector, starting with those of maximal symmetry.
k-SUBGROUPSMAG (52)	Provides all possible magnetic symmetries for a known space group of the paramagnetic phase and a set of one or more propagation vectors. Their group-subgroup hierarchy is also provided in a graphic form.
MAGNEXT (34)	Provides symmetry-forced systematic absences of nonpolarized neutron magnetic diffraction, along with the symmetry-adapted form of the magnetic structure factor, for any MSG or MSSG. Nonstandard settings are also supported.
MAGMODELIZE (56)	For any parent structure, provides the magnetic structure model corresponding to any MSG given by the user, as well as all domain-equivalent ones. It can be combined with k-SUBGROUPSMAG to explore all possible magnetic arrangements for a known propagation vector following a stepwise symmetry descent.
JANA2006 (47, 48)	General refinement program that includes a tool to construct for each *irrep* possible alternative models with their symmetries given by the possible *irrep* epikernels and kernel. It can deal both with commensurate and incommensurate structures. Magnetic structures can be uploaded or retrieved using magCIF files.
FULLPROF (12)	General refinement program that supports magCIF files both as input and output. A console application provides information on MSGs. Any MSG symmetry can be implemented in the model to be refined.

(*Continued*)

Table 6 (*Continued*)

Program or database	Program description
MVISUALIZE (45)	Online visualization using Jmol of any magnetic structure (commensurate or incommensurate) if uploaded as a magCIF file.
VESTA (27)	Visualization program that supports magnetic structures in magCIF format and magnetic symmetry (only commensurate structures).
Jmol (28)	Visualization program that supports magnetic structures (both commensurate and incommensurate) in magCIF format and magnetic symmetry.
MAGNDATA (22)	A collection of more than 250 magnetic structures (commensurate and incommensurate) described using magnetic symmetry and magCIF files.

Abbreviations: BNS, Belov-Neronova-Smirnova; *irrep*, irreducible representation; magCIF, extension of the crystallographic information file format to magnetic structures; MSG, magnetic space group; MSSG, magnetic superspace group; OG, Opechowski-Guccione.
[a]This is a summary of the most important free databases, computer tools, and programs for the analysis of magnetic structures that use (or are based on) magnetic symmetry.

MSSG $P11'(\alpha,\beta,\gamma)0s$; i.e., only the ubiquitous operation $\{1' \mid 0, 0, 0, 1/2\}$ is kept. This is the superspace symmetry of an arbitrary *mP2P3* modulation built up with all the *irrep* basis modes.

In simple cases such as the one above, the incommensurate spin configurations of higher symmetry are intuitively clear, and they are often tested in the refinements without appealing to concrete symmetry arguments. But for more general cases, the enumeration for a given *irrep* of distinct spin arrangements of higher symmetry is not obvious. The application of superspace symmetry allows the systematic exploration of these possible privileged configurations, distinguishing them from simplifying features that are not symmetry dictated. For an atom in a general position, the superspace symmetry of the phase does not restrict the form of its spin modulation, and it is only the relation of its (arbitrary) modulation with those of the other symmetry-related atoms in the average unit cell that is forced by the MSSG.

If the magnetic modulation is anharmonic or the magneto-structural coupling is strong enough to induce a structural modulation, the knowledge of the superspace symmetry of the magnetic phase is especially important, as it dictates the features of all induced effects. For *1k* structures, the presence of the superspace symmetry operation $\{1' \mid 0, 0, 0, 1/2\}$ in the MSSG ensures that the spin modulation can only have odd harmonics, whereas any magnetically induced structural modulation is restricted to even harmonics of the primary propagation vector. Hence, the existence of this very simple superspace symmetry operation is the reason for this general property satisfied by magnetically induced structural modulations. Higher harmonics of both the spin and the structural modulation are subject to the same MSSG as the first harmonic, but this in general implies transformation properties corresponding to *irreps* different from the one of the first harmonic. For instance, for the case of $RbFe(MoO_4)_2$ under the trigonal MSSG $P31'(1/3, 1/3, \gamma)ts$, the presence of the symmetry operation $\{3^+ \mid 0, 0, 0, 1/3\}$ not only enforces the helical spin arrangement for the first harmonic but also restricts the third harmonic (actually all $3n$ harmonics) to be a modulation with the spin component along c, i.e., an *mP1* distortion. Similarly, any induced structural distortion should comply with the MSSG, and this means specific restrictions on each induced harmonic modulation. For instance, the Fe atoms can suffer a displacive modulation with wave vector $2\mathbf{k}$, but it is restricted to the *ab* plane (82).

Conversely, if the paramagnetic phase is itself incommensurate owing to a structural modulation, the symmetry of the paramagnetic phase is then given by a gray superspace group, and the propagation vector of the magnetic ordering can be commensurate with the incommensurate wave

vector of the structural modulation. The MSSG of the magnetic phase is then related directly to the one of the paramagnetic phase (86).

5. CONCLUSIONS

Various computational tools developed during the past few years have made possible the relatively simple, systematic, and comprehensive application of magnetic symmetry in the analysis of magnetic structures, both commensurate and incommensurate. In the incommensurate case, the symmetry constraints of these phases are efficiently described and handled using superspace symmetry concepts with the introduction of MSSGs. A principle of maximal symmetry underlies most of the observed magnetic structures and their traditional description using *irreps*. The new computational instruments go beyond the traditional representation method and exploit the symmetry hierarchy among possible ordering models, such that a full characterization of the relevant symmetry breaking becomes a straightforward process. We have outlined this novel scenario by reviewing several examples and explaining the main concepts involved. We hope to have clearly shown that the representation method and a symmetry-based description of magnetic structures should be considered as complementary, and not alternative, approaches. The assignment of a magnetic symmetry in the form of an MSG or MSSG is not equivalent to the assignment of an *irrep*, except for 1-D *irreps*. Also, contrary to common belief, the assignment of an *irrep*, if multidimensional, generally introduces fewer constraints than an MSG. In complex situations, the most appropriate approach is a comprehensive application of both magnetic symmetry and *irrep* modes, and this is facilitated by the computational tools reviewed here and summarized in **Table 6**.

DISCLOSURE STATEMENT

The authors are not aware of any affiliations, memberships, funding, or financial holdings that might be perceived as affecting the objectivity of this review.

ACKNOWLEDGMENTS

The authors thank Vaclav Petricek, Juan Rodriguez-Carvajal, Branton Campbell, and Harold Stokes for helpful comments, their permanent receptivity to suggestions regarding their programs, and their efforts to achieve a common communication format. We are also very grateful to Koichi Momma and Robert Hanson for adapting their visualization programs to this format and in this way joining the endeavor for a robust and unambiguous communication of magnetic structures. This work has been supported by the Spanish Ministry of Science and Innovation (project MAT2012-34740) and the Government of the Basque Country (project IT779-13).

LITERATURE CITED

1. Koptsik VA. 1966. *Shubnikov Groups. Handbook on the Symmetry and Physical Properties of Crystal Structures.* Moscow: Moscow Univ. Press. In Russian
2. Bradley CJ, Cracknell AP. 1972. *The Mathematical Theory of Symmetry in Solids*. Oxford, UK: Clarendon
3. Perez-Mato JM, Ribeiro JL, Petricek V, Aroyo MI. 2012. Magnetic superspace groups and symmetry constraints in incommensurate magnetic phases. *J. Phys. Condens. Matter*. 24:163201
4. Petříček V, Fuksa J, Dušek M. 2010. Magnetic space and superspace groups, representation analysis: competing or friendly concepts? *Acta Crystallogr. Sect. A* 66:649–55
5. Janner A, Janssen T. 1980. Symmetry of incommensurate crystal phases. I. Commensurate basic structures. *Acta Crystallogr. Sect. A* 36:399–408

6. Bertaut EF. 1968. Representation analysis of magnetic structures. *Acta Crystallogr. Sect. A* 24:217–31
7. Bertaut EF. 1971. Magnetic structure analysis and group theory. *J. Phys. Colloques* 32:C1-462–70
8. Izyumov YA, Naish VE. 1979. Symmetry analysis in neutron diffraction studies of magnetic structures: 1. A phase transition concept to describe magnetic structures in crystals. *J. Magn. Magn. Mater.* 12:239–48
9. Izyumov YA, Naish VE, Ozerov RP. 1991. *Neutron Diffraction of Magnetic Materials*. Dordrecht, Neth.: Kluwer Acad.
10. Izyumov YA, Naish VE, Syromiatnikov VN. 1979. Symmetry analysis in neutron diffraction studies of magnetic structures: 2. Changes in periodicity at magnetic phase transitions. *J. Magn. Magn. Mater.* 12:249–61
11. Izyumov YA, Naish VE, Petrov SB. 1979. Symmetry analysis in neutron diffraction studies of magnetic structures: 3. An example: the magnetic structure of spinels. *J. Magn. Magn. Mater.* 13:267–74
12. Rodríguez-Carvajal J. 1993. Recent advances in magnetic structure determination by neutron powder diffraction. *Physica B* 192:55–69
13. Wills AS. 2000. A new protocol for the determination of magnetic structures using simulated annealing and representational analysis (SARA*b*). *Physica B* 276–78:680–81
14. Sikora W, Białas F, Pytlik L. 2004. MODY: a program for calculation of symmetry-adapted functions for ordered structures in crystals. *J. Appl. Crystallogr.* 37:1015–19
15. Dul M, Lesniewska B, Oles A, Pytlik L, Sikora W. 1997. Computer database of magnetic structures determined by neutron diffraction. *Physica B* 234–36:790–91
16. Schmid H. 2008. Some symmetry aspects of ferroics and single phase multiferroics. *J. Phys. Condens. Matter* 20:434201
17. Fiebig M. 2005. Revival of the magnetoelectric effect. *J. Phys. D* 38:R123–52
18. Johnson RD, Radaelli PG. 2014. Diffraction studies of multiferroics. *Annu. Rev. Mater. Res.* 44:269–98
19. Kimura T. 2007. Spiral magnets as magnetoelectrics. *Annu. Rev. Mater. Res.* 37:387–413
20. Hall SR, Allen FH, Brown ID. 1991. The Crystallographic Information File (CIF): a new standard archive file for crystallography. *Acta Crystallogr. Sect. A* 47:655–85
21. Int. Union Crystallogr. 2015. *Commission on Magnetic Structures.* **http://www.iucr.org/iucr/commissions/magnetic-structures**
22. Bilbao Crystallogr. Serv. 2014. MAGNDATA: a collection of magnetic structures with portable cif-type files. *Bilbao Crystallographic Server.* **http://www.cryst.ehu.es/magndata/**
23. Aroyo MI, Perez-Mato JM, Capillas C, Kroumova E, Ivantchev S, et al. 2006. Bilbao Crystallographic Server: I. Databases and crystallographic computing programs. *Z. Krist.* 221 1:15–27
24. Aroyo MI, Kirov A, Capillas C, Perez-Mato JM, Wondratschek H. 2006. Bilbao Crystallographic Server: II. Representations of crystallographic point groups and space groups. *Acta Crystallogr. Sect. A* 62:115–28
25. Glazer AM, Aroyo MI, Authier A. 2014. Seitz symbols for crystallographic symmetry operations. *Acta Crystallogr. Sect. A* 70:300–2
26. Wondratschek H, Müller U, eds. 2011. *International Tables for Crystallography*, Vol. A1: *Symmetry Relations Between Space Groups*. Dordrecht, Neth.: Kluwer Acad. **http://it.iucr.org/A1/**
27. Momma K, Izumi F. 2011. *VESTA 3* for three-dimensional visualization of crystal, volumetric and morphology data. *J. Appl. Crystallogr.* 44:1272–76
28. Hanson R. 2013. *Jmol: an open-source Java viewer for chemical structures in 3D*. **http://www.jmol.org/**
29. Litvin DB. 2013. *Magnetic Group Tables: 1-, 2- and 3-Dimensional Magnetic Subperiodic Groups and Magnetic Space Groups*. Chester, UK: Int. Union Crystallogr. **http://www.iucr.org/publ/978-0-9553602-2-0**
30. Hahn T, ed. 2002. *International Tables for Crystallography*, Vol. A: *Space-Group Symmetry*. Dordrecht, Neth.: Kluwer Acad. 5th ed.
31. Opechowski W, Guccione R. 1965. Magnetic symmetry. In *Magnetism*, Vol. II, Part A, ed. GT Rado, H Suhl, pp. 105–65. New York: Academic
32. Belov NV, Neronova NN, Smirnova TS. 1957. Shubnikov groups. *Sov. Phys. Crystallogr.* 2:311–22
33. Stokes HT, Campbell BJ. 2011. ISO-MAG: table of magnetic space groups. *ISOTROPY Software Suite.* **http://iso.byu.edu**
34. Gallego SV, Tasci ES, de la Flor G, Perez-Mato JM, Aroyo MI. 2012. Magnetic symmetry in the Bilbao Crystallographic Server: a computer program to provide systematic absences of magnetic neutron diffraction. *J. Appl. Crystallogr.* 45:1236–47

35. Lee N, Vecchini C, Choi YJ, Chapon LC, Bombardi A, et al. 2013. Giant tunability of ferroelectric polarization in $GdMn_2O_5$. *Phys. Rev. Lett.* 110:137203
36. FIZ Karlsruhe. 2014. *ICSD: Inorganic Crystal Structure Database*. Eggenstein-Leopoldshafen, Ger. **http://icsd.fiz-karlsruhe.de**
37. Kagomiya I, Kohn K, Uchiyama T. 2002. Structure and ferroelectricity of RMn_2O_5. *Ferroelectrics* 280:131–43
38. Bilbao Crystallogr. Serv. 2014. IDENTIFY GROUP: identification of a space group from a set of generators in an arbitrary setting. *Bilbao Crystallographic Server*. **http://www.cryst.ehu.es/cryst/identify_group**
39. Bilbao Crystallogr. Serv. 2014. IDENTIFY MAGNETIC GROUP: identification of a magnetic space group from a set of generators in an arbitrary setting. *Bilbao Crystallographic Server*. **http://www.cryst.ehu.es/cryst/identify_mgroup**
40. Doubrovsky C, André G, Gukasov A, Auban-Senzier P, Pasquier CR, et al. 2012. Magnetic phase transitions in $PrMn_2O_5$: Importance of ion-size threshold size effects in RMn_2O_5 compounds (R = rare earth). *Phys. Rev. B* 86:174417
41. Stokes HT, Campbell BJ. 2014. ISOCIF: create or modify CIF files. *ISOTROPY Software Suite*. **http://iso.byu.edu**
42. Bilbao Crystallogr. Serv. 2014. STRCONVERT: structure data converter & editor. *Bilbao Crystallographic Server*. **http://www.cryst.ehu.es/cryst/strconvert**
43. Stokes HT, Campbell BJ. 1998. FINDSYM: identify the space group of a crystal, given the positions of the atoms in a unit cell. *ISOTROPY Software Suite*. **http://iso.byu.edu**
44. Kresse G, Furthmüller J. 1996. Efficient iterative schemes for ab initio total-energy calculations using a plane-wave basis set. *Phys. Rev. B* 54:11169–86
45. Bilbao Crystallogr. Serv. 2014. MVISUALIZE: 3D visualization of magnetic structures with Jmol. *Bilbao Crystallographic Server*. **http://www.cryst.ehu.es/cryst/mvisualize**
46. Bilbao Crystallogr. Serv. 2013. MAXMAGN: maximal magnetic space groups for a given a propagation vector and resulting magnetic structural models. *Bilbao Crystallographic Server*. **http://www.cryst.ehu.es/cryst/maxmagn**
47. Petricek V, Dusek M, Palatinus L. 2006. *Jana2006: The Crystallographic Computing System*. **http://jana.fzu.cz/**
48. Petříček V, Dušek M, Palatinus L. 2014. Crystallographic computing system JANA2006: general features. *Z. Krist.* 229(5):345–52
49. Muñoz A, Casais MT, Alonso JA, Martinez-Lope MJ, Martinez JL, et al. 2001. Complex magnetism and magnetic structures of the metastable $HoMnO_3$ perovskite. *Inorg. Chem.* 40:1020–28
50. Lee N, Choi YJ, Ramazanoglu M, Ratcliff W, Kiryukhin V, Cheong SW. 2011. Mechanism of exchange striction of ferroelectricity in multiferroic orthorhombic $HoMnO_3$ single crystals. *Phys. Rev. B* 84:020101
51. Fu Z, Zheng Y, Xiao Y, Bedanta S, Senyshyn A, et al. 2013. Coexistence of magnetic order and spin-glass-like phase in the pyrochlore antiferromagnet $Na_3Co(CO_3)_2Cl$. *Phys. Rev.* 87:214406
52. Bilbao Crystallogr. Serv. 2014. k-SUBGROUPSMAG: magnetic subgroups consistent with some given propagation vector(s) or a supercell. *Bilbao Crystallographic Server*. **http://www.cryst.ehu.es/cryst/k_subgroupsmag**
53. Ressouche E, Kernavanois N, Regnault LP, Henry JY. 2006. Magnetic structures of the metal monoxides NiO and CoO re-investigated by spherical neutron polarimetry. *Physica B* 385–86:394–97
54. Herrmann-Ronzaud D, Burlet P, Rossat-Mignod J. 1978. Equivalent type-II magnetic structures: CoO, a collinear antiferromagnet. *J. Phys. C: Solid State Phys.* 11:2123–37
55. Jauch W, Reehuis M, Bleif HJ, Kubanek F, Pattison P. 2001. Crystallographic symmetry and magnetic structure of CoO. *Phys. Rev. B* 64:052102
56. Bilbao Crystallogr. Serv. 2014. MAGMODELIZE: magnetic structure models for any given magnetic symmetry. *Bilbao Crystallographic Server*. **http://www.cryst.ehu.es/cryst/magmodelize**
57. Zhao LL, Wu S, Wang JK, Hodges JP, Broholm C, Morosan E. 2013. Quasi-two-dimensional non-collinear magnetism in the Mott insulator $Sr_2F_2Fe_2OS_2$. *Phys. Rev. B* 87:020406
58. Aroyo MI, Orobengoa D, de la Flor G, Perez-Mato JM, Wondratschek H. 2014. Brillouin-zone databases on the Bilbao Crystallographic Server. *Acta Crystallogr. Sect. A* 70:126–37

59. Chattopadhyay T, Brown PJ, Roessli B, Stepanov AA, Barilo SN, Zhigunov DI. 1992. Magnetic ordering of Cu in Gd_2CuO_4. *Phys. Rev. B* 46:5731–34
60. Perez-Mato JM, Aroyo MI, García A, Blaha P, Schwarz K, et al. 2004. Competing structural instabilities in the ferroelectric Aurivillius compound $SrBi_2Ta_2O_9$. *Phys. Rev. B* 70:214111
61. Etxebarria I, Perez-Mato JM, Boullay P. 2010. The role of trilinear couplings in the phase transitions of Aurivillius compounds. *Ferroelectrics* 401:17–23
62. Ghosez P, Triscone JM. 2011. Multiferroics: coupling of three lattice instabilities. *Nat. Mater.* 10:269–70
63. Quintero M, Morocoima M, Guerrero E, Ruiz J. 1994. Temperature variation of lattice parameters and thermal expansion coefficients of the compound $MnGa_2Se_4$. *Phys. Status Solidi A* 146:587–93
64. Opechowski W, Dreyfus T. 1971. Classifications of magnetic structures. *Acta Crystallogr. Sect. A* 27:470–84
65. Opechowski W. 1971. Analyse des structures magnétiques et théorie des groupes: on two classifications of magnetic structures. *J. Phys. Colloques* 32:C1-457–61
66. Opechowski W, Litvin DB. 1977. Error corrections corrected, remarks on Bertaut's article "Simple derivation of magnetic space groups". *Ann. Phys.* 2:121–25
67. Campbell BJ, Stokes HT, Tanner DE, Hatch DM. 2006. *ISODISPLACE*: a web-based tool for exploring structural distortions. *J. Appl. Crystallogr.* 39:607–14. **http://stokes.byu.edu/isodistort.html**
68. Ascher E. 1977. Permutation representations, epikernels and phase transitions. *J. Phys. C Solid State Phys.* 10:1365–77
69. de Wolff PM. 1974. The pseudo-symmetry of modulated crystal structures. *Acta Crystallogr. Sect. A* 30:777–85
70. Janner A, Janssen T. 1980. Symmetry of incommensurate crystal phases. II. Incommensurate basic structure. *Acta Crystallogr. Sect. A* 36:408–15
71. Janssen T, Janner A. 2014. Aperiodic crystals and superspace concepts. *Acta Crystallogr. Sect. B* 70:617–51
72. Janssen T, Janner A, Looijenga-Vos A, de Wolff PM. 2006. Incommensurate and commensurate modulated structures. In *International Tables for Crystallography*, Vol. C: *Mathematical, Physical and Chemical Tables*, ed. E. Prince, pp. 907–55. Dordrecht, Neth.: Kluwer Acad.
73. Janssen T, Chapuis G, de Boissieu M. 2007. *Aperiodic Crystals: From Modulated Phases to Quasicrystals*. IUCr Monogr. Crystallogr. No. 20. Oxford, UK: Oxford Univ. Press
74. Van Smaalen S. 2007. *Incommensurate Crystallography*. IUCr Monogr. Crystallogr. No. 21. Oxford, UK: Oxford Univ. Press
75. Schobinger-Papamantellos P, Janssen T. 2006. The symmetry of the incommensurate magnetic phase of $ErFe_4Ge_2$. *Z. Krist.* 221:732–34
76. Schönleber A, van Smaalen S, Palatinus L. 2006. Structure of the incommensurate phase of the quantum magnet TiOC. *Phys. Rev. B* 73:214410
77. Slawinski W, Przenioslo R, Sosnowska I, Bieringer M, Margiolaki I, Suard E. 2009. Modulation of atomic positions in $CaCu_xMn_{7-x}O_{12}$ ($x < 0.1$). *Acta Crystallogr. Sect. B* 65:535–42
78. Meddar L, Josse M, Deniard P, La C, Andre G, et al. 2009. Effect of nonmagnetic substituents Mg and Zn on the phase competition in the multiferroic antiferromagnet $MnWO_4$. *Chem. Mater.* 21:5203–14
79. Ribeiro JL, Vieira LG. 2010. Landau model for the phase diagrams of the orthorhombic rare-earth manganites $RMnO_3$ (R = Eu, Gd, Tb, Dy, Ho). *Phys. Rev. B* 82:064410
80. Ribeiro JL. 2010. Symmetry, incommensurate magnetism and ferroelectricity: the case of the rare-earth manganites $RMnO_3$. *J. Phys. Conf. Ser.* 226:012013
81. Janoschek M, Fischer P, Schefer J, Roessli B, Pomjakushin V, et al. 2010. Single magnetic chirality in the magnetoelectric $NdFe_3(^{11}BO_3)_4$. *Phys. Rev. B* 81:094429
82. Ribeiro JL, Perez-Mato JM. 2011. Symmetry and magnetic field driven transitions in the 2D triangular lattice compound $RbFe(MoO_4)_2$. *J. Phys. Condens. Matter* 23:446003
83. Abakumov AM, Tsirlin AA, Perez-Mato JM, Petříček V, Rosner H, et al. 2011. Spiral ground state against ferroelectricity in the frustrated magnet $BiMnFe_2O_6$. *Phys. Rev. B* 83:214402
84. Urcelay-Olabarria I, Perez-Mato JM, Ribeiro JL, García-Muñoz JL, Ressouche E, et al. 2013. Incommensurate magnetic structures of multiferroic $MnWO_4$ studied within the superspace formalism. *Phys. Rev. B* 87:014419
85. Terada N, Khalyavin DD, Perez-Mato JM, Manuel P, Prabhakaran D, et al. 2014. Magnetic and ferroelectric orderings in multiferroic α-$NaFeO_2$. *Phys. Rev. B* 89:184421

86. Prokeš K, Petříček V, Ressouche E, Hartwig S, Ouladdiaf B, et al. 2014. (3 + 1)-dimensional crystal and antiferromagnetic structures in CeRuSn. *J. Phys. Condens. Matter* 26:122201
87. Orlandi F, Righi L, Ritter C, Pernechele C, Solzi M, et al. 2014. Superspace application on magnetic structure analysis of the Pb_2MnWO_6 double perovskite system. *J. Mater. Chem. C* 2:9215–23
88. Herpin A, Meriel P. 1961. Étude de l'antiferromagnétisme helicoidal de $MnAu_2$ par diffraction de neutrons. *J. Phys. Radium.* 22:337–48
89. Brown ID, McMahon B. 2002. CIF: the computer language of crystallography. *Acta Crystallogr. Sect. B* 58:317–24
90. Laffargue D, Fourgeot F, Bourée F, Chevalier B, Roisnel T, et al. 1996. The antiferromagnetic-ferromagnetic transition of $Ce_2Pd_{2.04}Sn_{0.96}$ stannide. *Solid State Commun.* 100:575–79
91. Rodríguez-Carvajal J, Bourée F. 2012. Symmetry and magnetic structures. *EPJ Web Conf.* 22:00010
92. Biffin A, Johnson RD, Choi S, Freund F, Manni S, et al. 2014. Unconventional magnetic order on the hyperhoneycomb Kitaev lattice in β-Li_2IrO_3: full solution via magnetic resonant X-ray diffraction. *Phys. Rev. B* 90:205116
93. Kenzelmann M, Lawes G, Harris AB, Gasparovic G, Broholm C, et al. 2007. Direct transition from a disordered to a multiferroic phase on a triangular lattice. *Phys. Rev. Lett.* 98:267205